Magnetic Resonance Electrical Impedance Tomography (MREIT)

Hyung Joong Kim

Impedance Imaging Research Center (IIRC)

Department of Biomedical Engineering

Kyung Hee University, KOREA

Contents

- Introduction and Motivation
- Electrical Impedance Tomography (EIT)
- Magnetic Resonance Electrical Impedance Tomography (MREIT)
  - Basics and requirements
  - Agar phantom experiments
  - Tissue phantom experiments
  - Animal experiments
- Application & summary

Volume Conductor Field

- Conductivity, σ
- Internal current source, *f*
- External injection current, *I*
- Geometry (boundary shape and size)
- Measurable quantities
  - Boundary voltage and limited internal voltage
  - Boundary or exit current and limited internal current
  - External and/or internal magnetic flux density

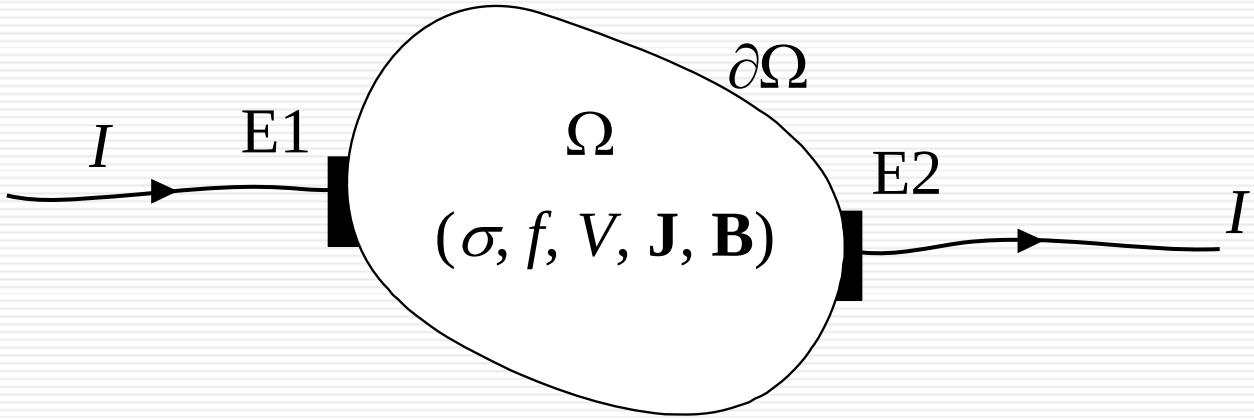

Volume Conductor Field

- White lines are current stream lines.
- Black lines are equipotential lines.

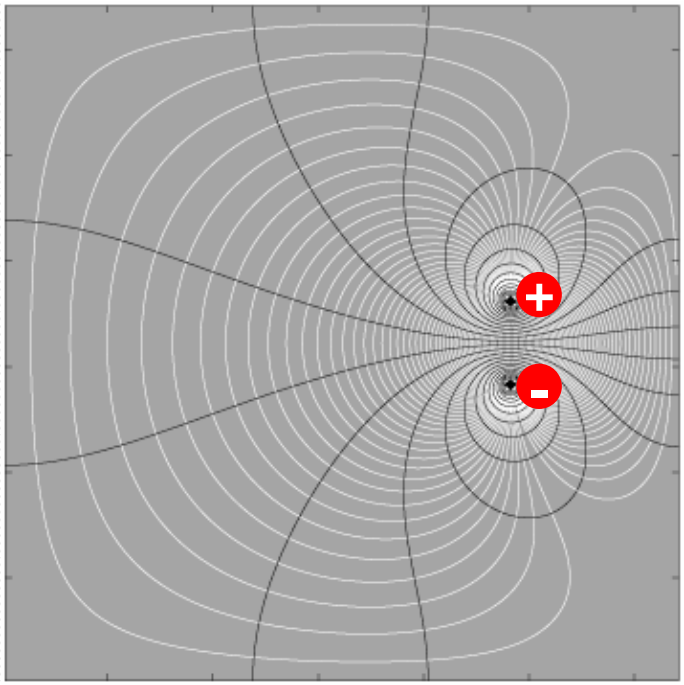

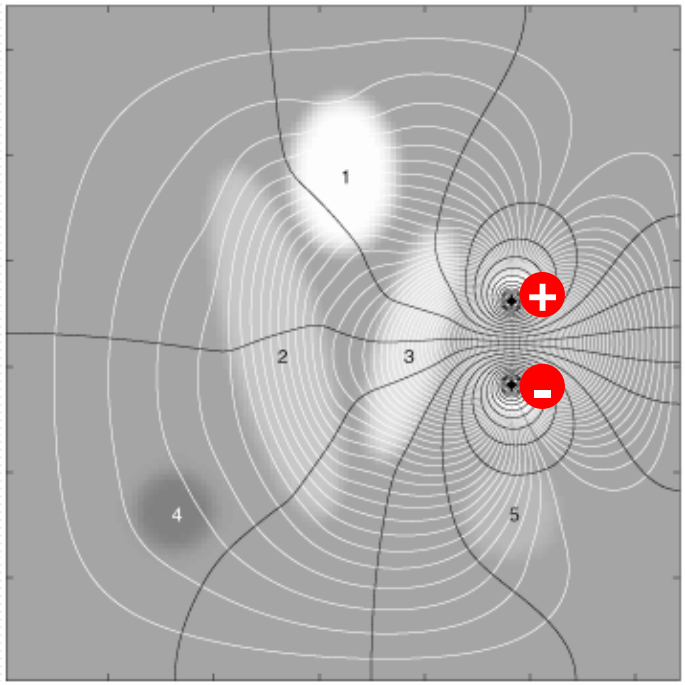

$$\nabla \cdot (\sigma \nabla V) = -f \qquad -\sigma \frac{\partial V}{\partial n} = 0 \ \text{ on } \partial\Omega \qquad \boldsymbol{J} = -\sigma \nabla V$$

Bio-electric Signal

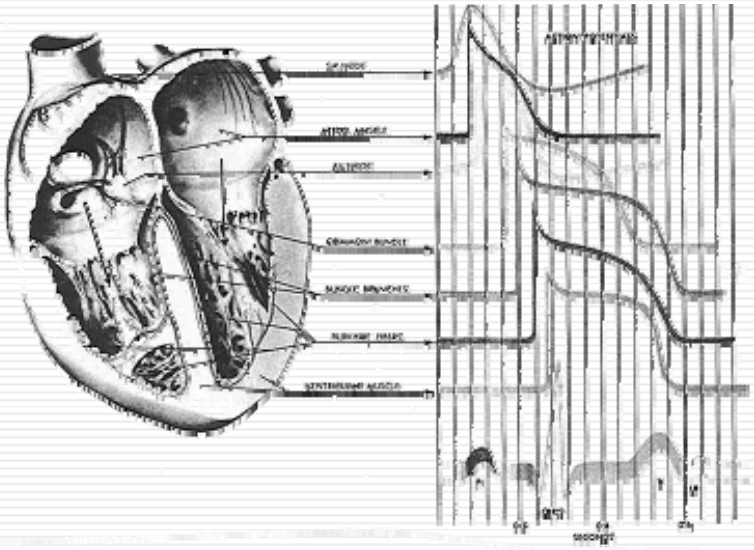

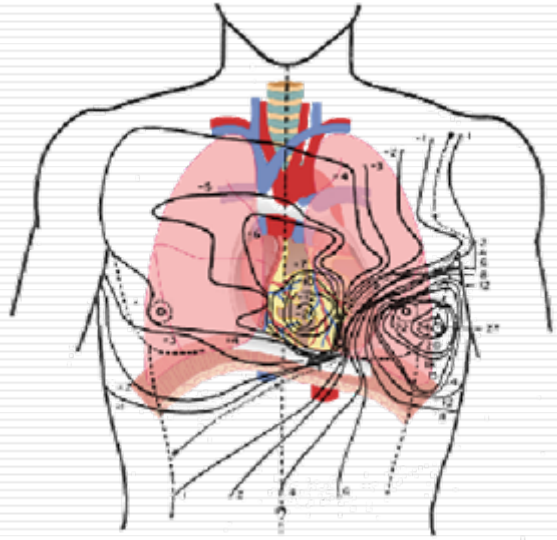

$$\nabla \cdot \left(\sigma(\boldsymbol{r};t) \nabla V(\boldsymbol{r};t) \right) = -f(\boldsymbol{r};t)$$

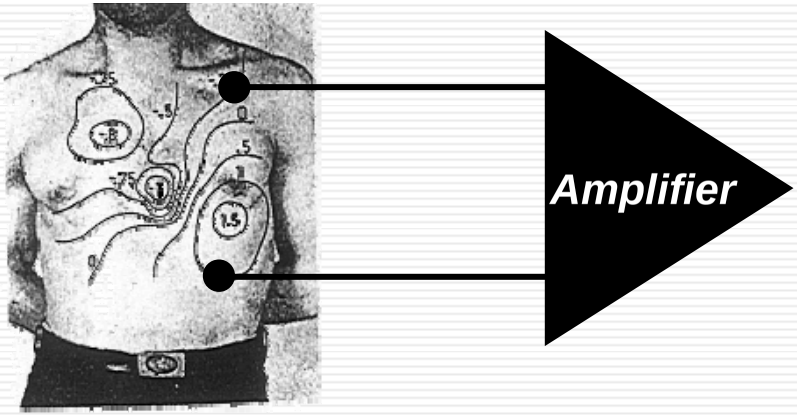

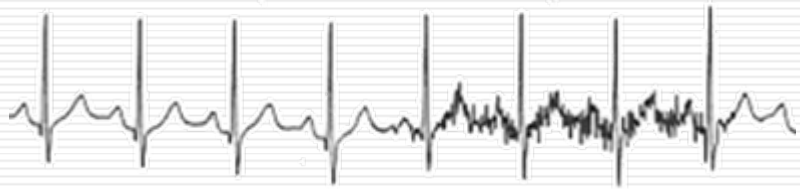

ECG

Medical Instrumentation: Application and Design, 3rd ed., by J. G. Webster

Bio-magnetic Signal

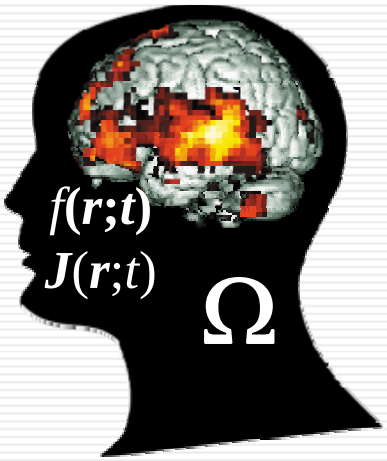

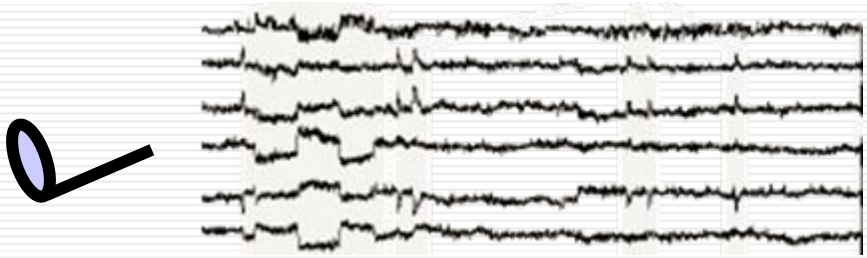

MEG

$$\boldsymbol{B}(\boldsymbol{r};t)=\frac{\mu_0}{4\pi}\int_{\Omega}\boldsymbol{J}(\boldsymbol{r}';t)\times\frac{\boldsymbol{r}-\boldsymbol{r}'}{\left|\boldsymbol{r}-\boldsymbol{r}'\right|^3}dv'$$

$$\nabla\cdot\left(\sigma(\boldsymbol{r};t)\nabla V(\boldsymbol{r};t)\right)=-f(\boldsymbol{r};t)$$

$$\boldsymbol{J}(\boldsymbol{r};t)=-\sigma(\boldsymbol{r};t)\nabla V(\boldsymbol{r};t)$$

Hepatic Tumor Conductivity

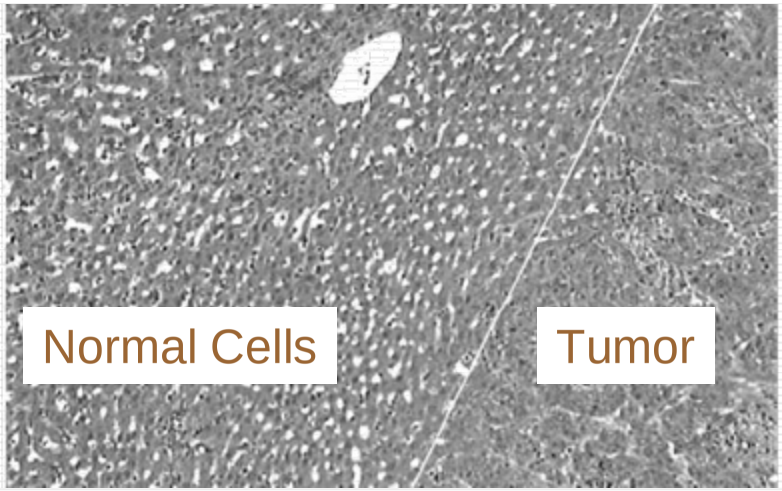

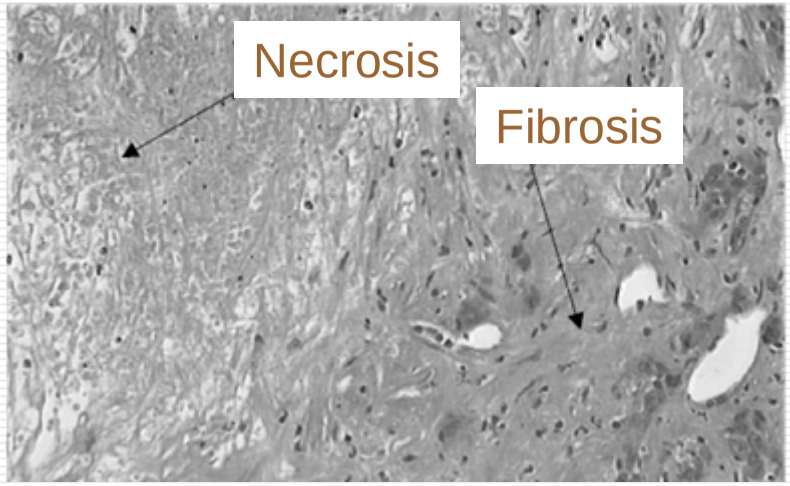

D. Haemmerich, S. T. Staelin, J. Z. Tsai, S. Tungjitkusolmun, D. M. Mahvi and J. G. Webster, "*In vivo* electrical conductivity of hepatic tumours," *Physiol. Meas.*, vol. 24, pp. 251–260, 2003.

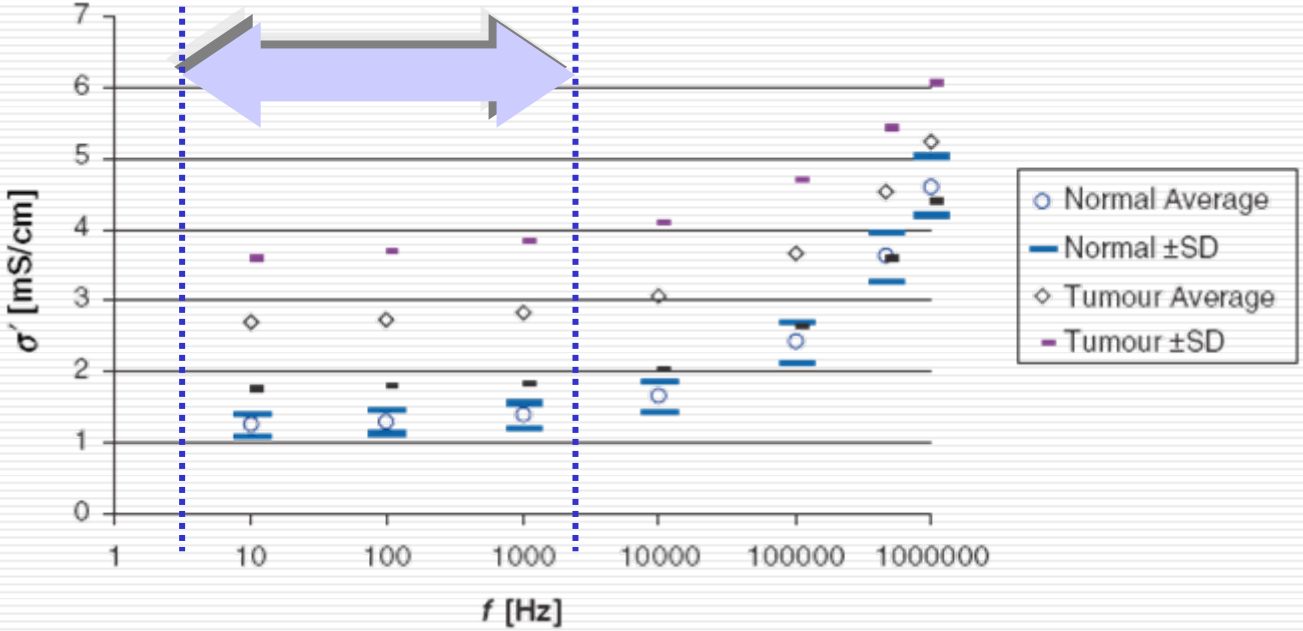

Breast Tumor Conductivity

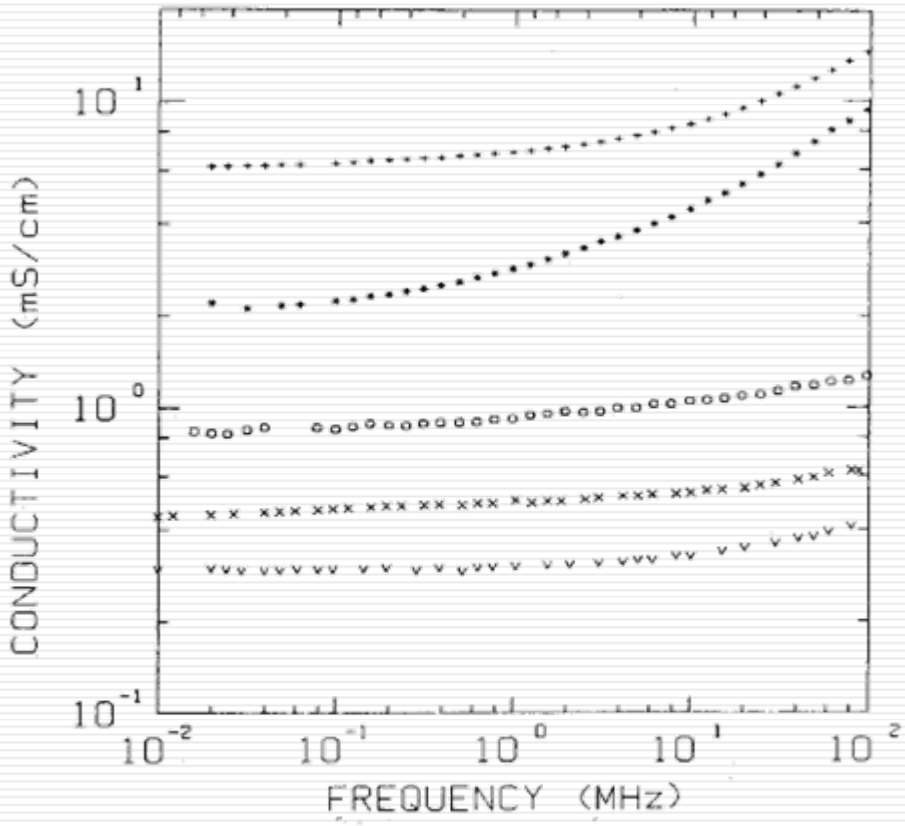

Fig. 3. Dielectric constant of breast carcinoma as a function of frequency. (*) sample *A*1, central part of tumor, (+) sample *A*3, tissue surrounding the tumor (○) sample *C*1, mainly fatty tissue containing infiltrating tumor cells, (x) peripheral sample (*G*3) located relatively far from central part of tumor, (v) normal (control) breast tissue.

Normal Tissue

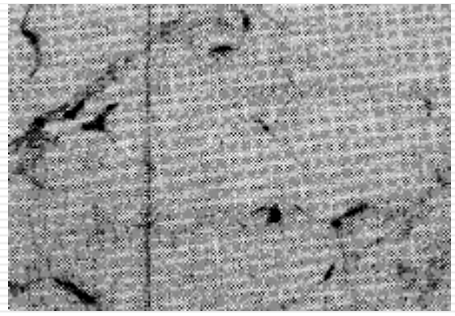

Lobular Carcinoma

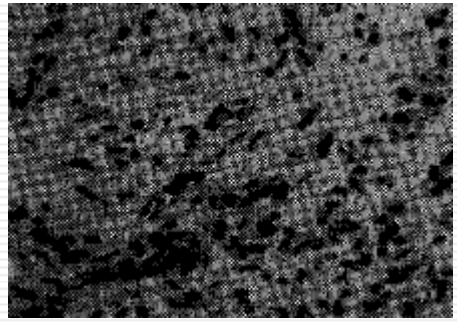

Ductal Carcinoma

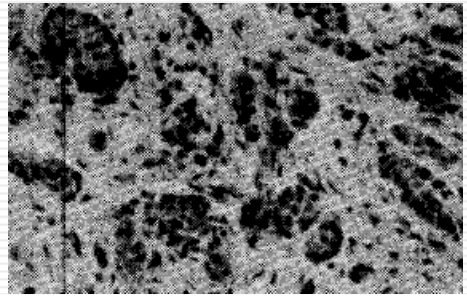

A. J. Surowiec, S. S. Stuchly, J. R. Barr, and A. Swarup, "Dielectric properties of breast carcinoma and the surrounding tissues," *IEEE Trans. Biomed. Eng.*, vol. 35, no. 4, pp. 257–263, 1988.

Conductivity and Neural Activity

- Cole K S and Curtis H J 1939 Electrical impedance of the squid giant axon during activity *J. Gen. Physiol.* 22 649-670
- Cole K S 1949 Dynamic electrical characteristics of squid axon membrane *Arch. Sci. Physiol.* 3 253-258
- Adey W, Kado R and Didio J 1962 Impedance measurements in brain tissue of animals using microvolt signals *Exp. Neruol.* 5 47-66
- Van-Harreveld A and Schade J 1962 Changes in the electrical conductivity of cerebral cortex during seizure activity *Exp. Neurol.* 5 383-400
- Rank J B 1963 Specific impedance of rabbit cerebral cortex *Exp. Neurol.* 7 144-152
- Aladjolova N A 1964 Slow electrical processes in the brain *Prog. Brain Res.* 7 155-237
- Geddes L A and Baker L E 1967 The specific resistance of biological material: a compendium of data for the biomedical engineer and physiologist *Med. Biol. Eng.* 5 271-293
- Meister M, Pine J, Baylor, DA 1994 Multi-neuronal signals from the retina: acquisition and analysis *J. Neurosci. Meth.* 51 95-106

Neural activity produces
3-5% local conductivity changes at low frequency.

Motivation and Goal

- Physiological functions and pathological changes alter conductivity values.
- Neural activity induces changes in conductivity.
- Source imaging needs conductivity values.
- Electromagnetic stimulations need conductivity values.

Cross-sectional Imaging of

Internal Conductivity

and Current Density Distribution

EIT using Boundary Measurements

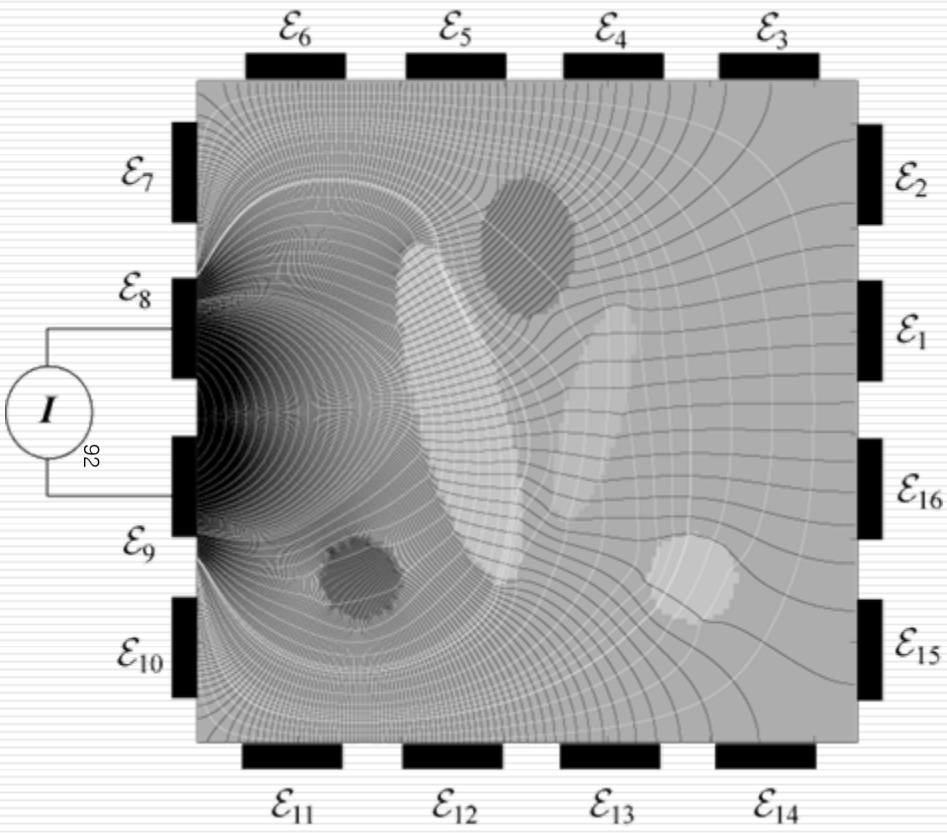

Neumann

(Boundary Current)

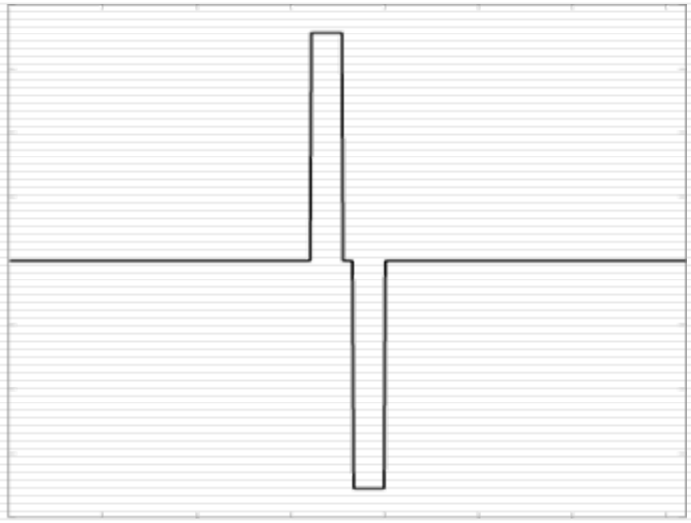

Dirichlet

(Boundary Voltage)

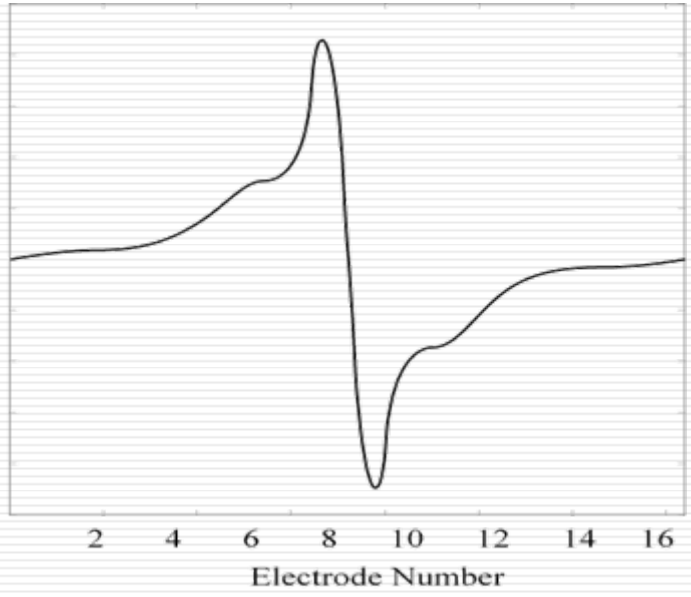

$$\nabla \cdot (\sigma \nabla V) = 0 \quad \text{in} \quad \Omega \qquad \nabla \cdot \mathbf{J} = 0$$

$$-\sigma \nabla V \cdot \mathbf{n} = g \quad \text{on} \quad \partial\Omega \qquad \mathbf{J} = -\sigma \nabla V$$

EIT Images: Thorax

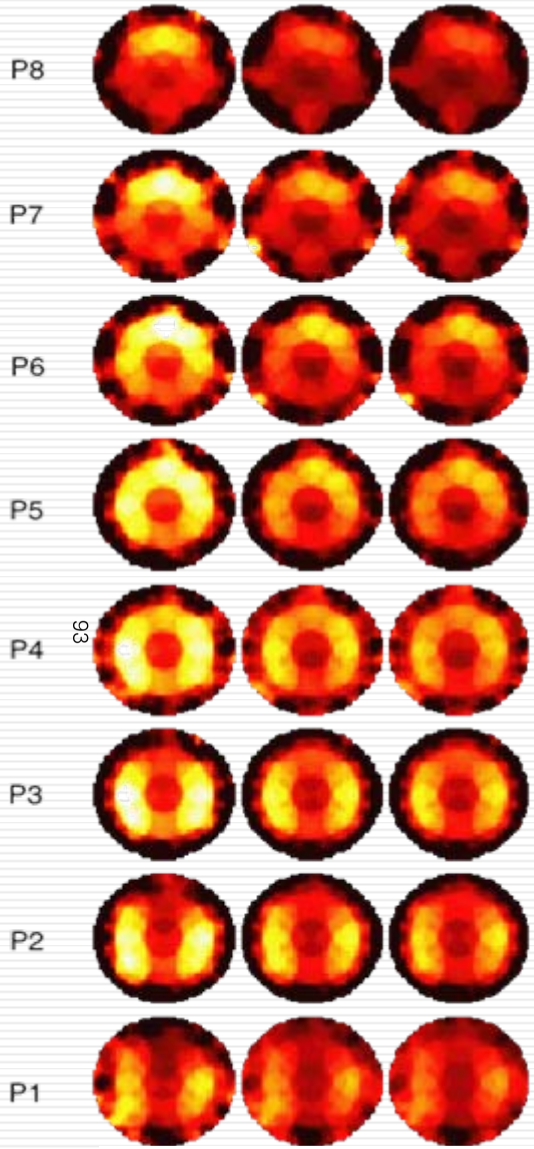

@RV @FRC @PTV (w.r.t TLC)

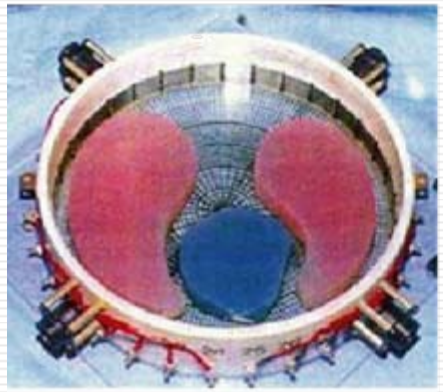

Phantom (Saline + Agar)

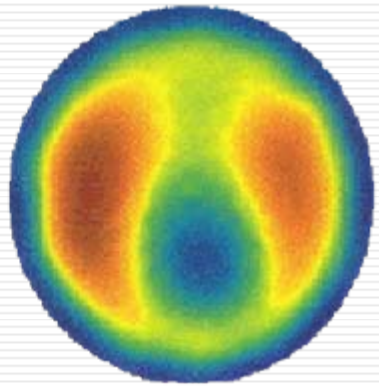

Static Image of ρ

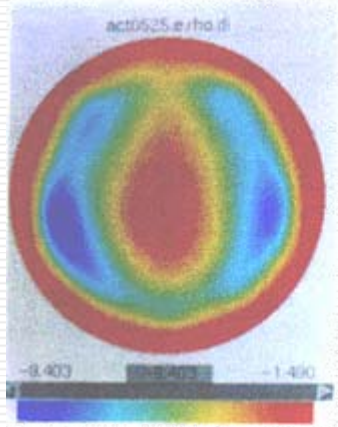

Thorax @ Expiration

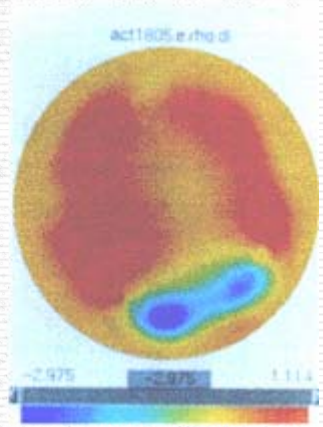

Thorax @ Inspiration

M. Cheney, D. Isaacson, and J. C. Newell, "Electrical impedance tomography," *SIAM Rev.*, vol. 41, pp. 85-101, 1999.

P. Metherall, D. C. barber, R. H. Smallwood, and B. H. Brown, "Three-dimensional electrical impedance tomography," *Nature*, vol. 380, pp. 509-512, 1996.

P. Metherall, *Three Dimensional Electrical Impedance Tomography of the Human Thorax*, PhD Thesis, Dept. of Med. Phys. And Clin. Eng., Univ. of Sheffield, Sheffield, UK, 1998.

EIT Images: Brain

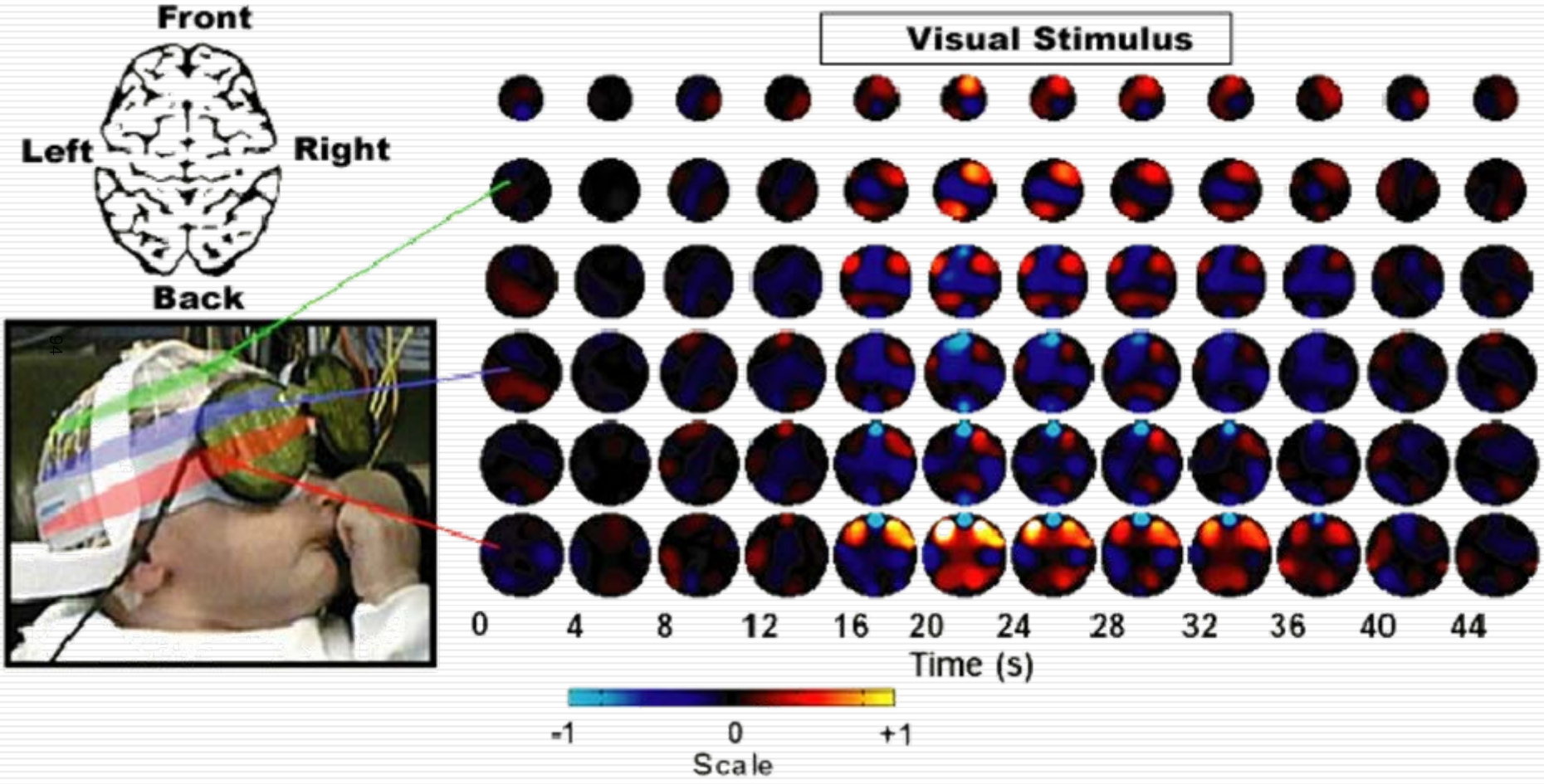

A. T. Tidswell, A. Gibson, R. H. Bayford, and D. S. Holder, “Three-dimensional electrical impedance tomography of human brain activity,” *NeuroImage*, vol. 13, pp. 283-294, 2001.

Static Imaging with High Spatial Resolution

- Internal measurements
- Non-invasive measurements
- Non-contact measurements
- Spatial information encoded in measured data

Magnetic Resonance Electrical Impedance Tomography (MREIT)

Internal magnetic flux density measurements using MRI

Reconstruct cross-sectional images of conductivity and current density distribution

How to Measure Magnetic Field?

- **Current injection MRI technique**
- **Originally developed for Current Density Imaging (CDI)**

M. L. G. Joy, G. C. Scott, and R. M. Henkelman, "*In vivo* detection of applied electric currents by magnetic resonance imaging," *Mag. Reson. Imag.*, vol. 7, pp. 89-94, 1989.

G. C. Scott, M. L. G. Joy, R. L. Armstrong, and R. M. Henkelman, "Measurement of nonuniform current density by magnetic resonance," *IEEE Trans. Med. Imag.*, vol. 10, no. 3, pp. 362-374, 1991.

Basics of MREIT Experiment

Experimental Setup

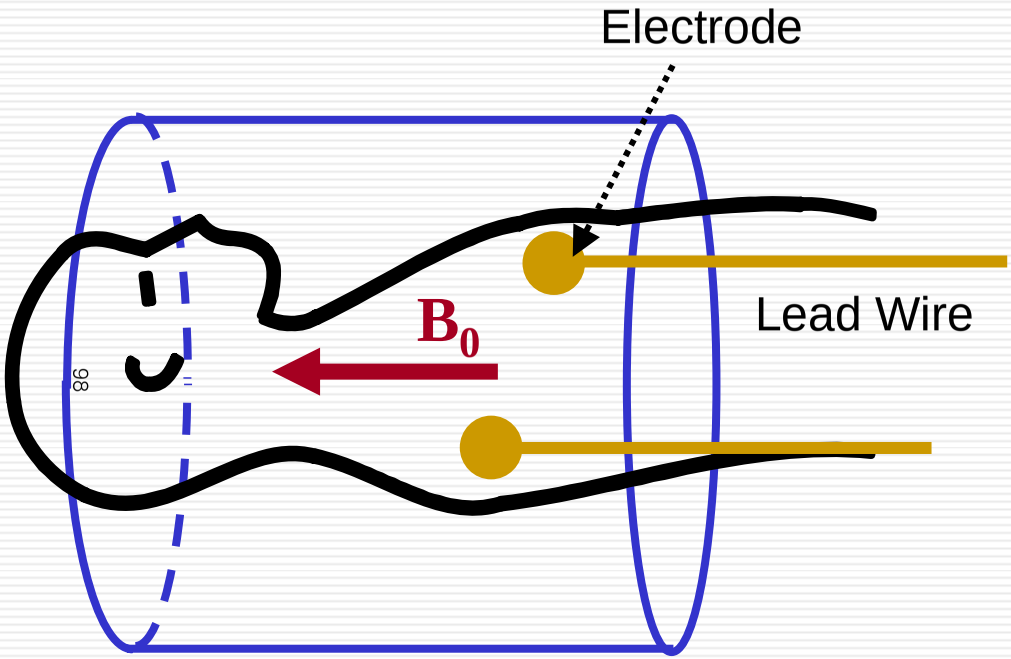

SE Pulse Sequence

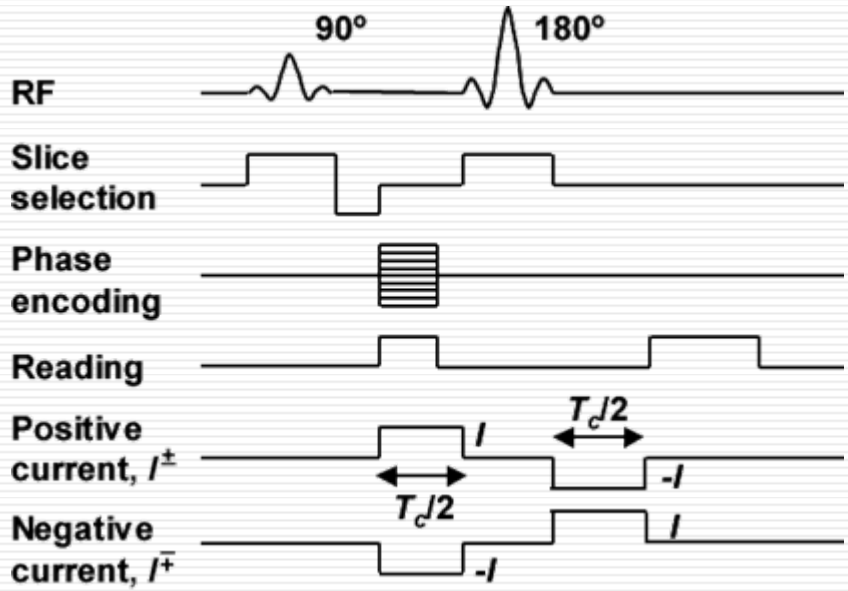

Raw Data

Magnitude Image

Phase Image

$$S_{q\pm}(m,n) = \int\int_{-\infty}^{\infty} M(x,y) e^{j\delta(x,y)} e^{\pm j\gamma B_q(x,y)T_c} e^{j(xm\Delta k_x + yn\Delta k_y)} dxdy$$

SE Pulse Sequence

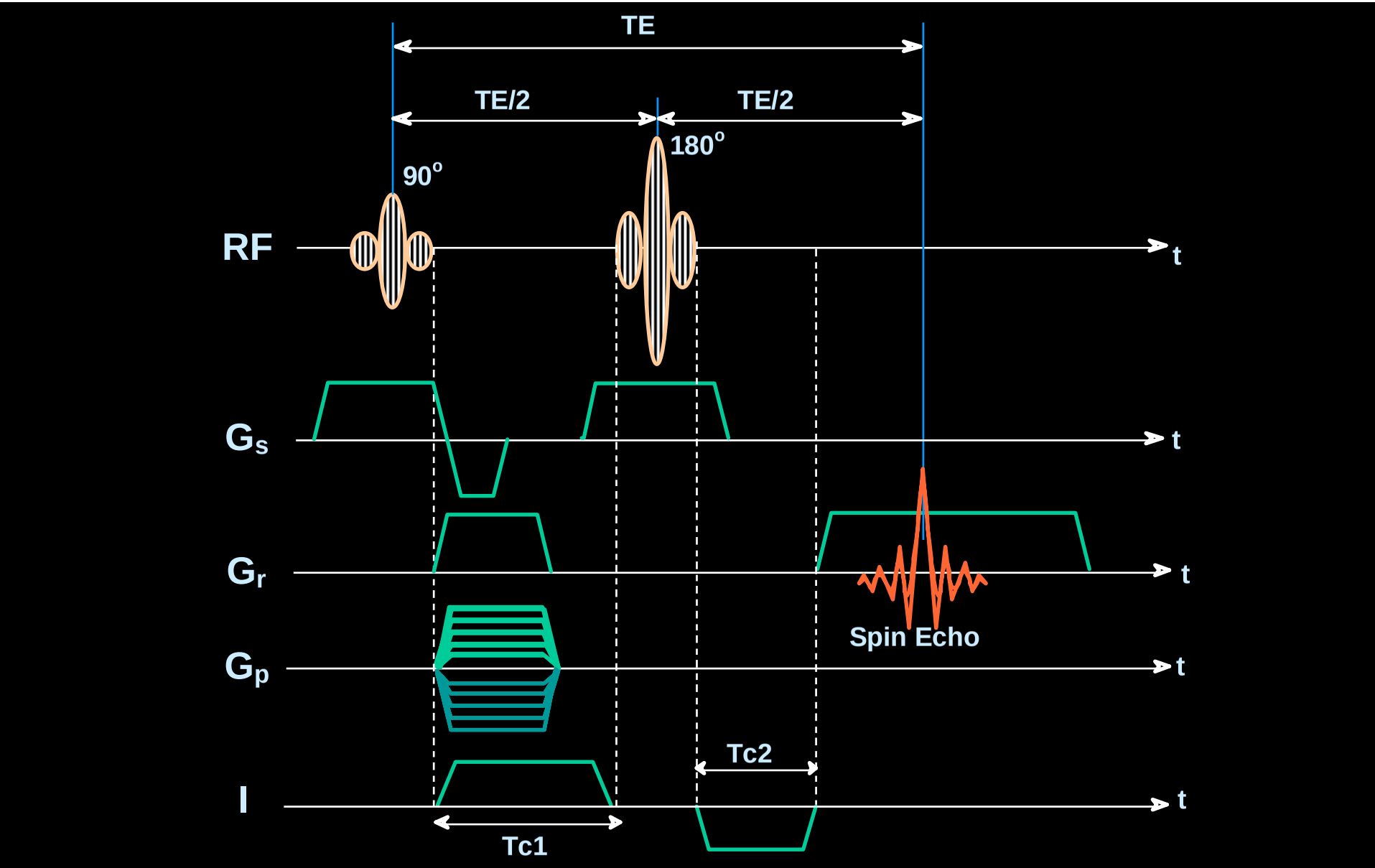

Magnetic Flux Density (B_z) Imaging

We use both positive and negative injection currents.

↓ k-space data collection

$$\mathcal{S}^{\pm}(m,n) = \int\int_{-\infty}^{\infty} M(x,y)e^{j\delta(x,y)}e^{\pm j\gamma B_z(x,y)T_c}e^{j(xm\Delta k_x + yn\Delta k_y)}dxdy$$

↓ Inverse Fourier Transform

$$\mathcal{M}^{\pm}(x,y) = M(x,y)e^{j\delta(x,y)}e^{\pm j\gamma B_z(x,y)T_c}$$

↓ Compute phase and unwrap phase

$$\Psi(x,y) = \arg\left(\frac{\mathcal{M}^{+}(x,y)}{\mathcal{M}^{-}(x,y)}\right) = 2\gamma B_z(x,y)T_c$$

↓ Scaling and slice ordering

$$B_z(x,y) = \frac{\Psi(x,y)}{2\gamma T_c} = \frac{1}{2\gamma T_c}\arg\left(\frac{\mathcal{M}^{+}(x,y)}{\mathcal{M}^{-}(x,y)}\right)$$

B_z-based Algorithms

- **Harmonic B_z Algorithm[1,2]**
- **Gradient B_z Decomposition Algorithm [3,4]**
- **Variational Gradient B_z Algorithm [5,6]**
- **Other Algorithms**
  - Multiple boundary voltage data
  - Hybrid algorithms
  - *A priori* structural information
  - Other new algorithms

(1) Seo *et al.*, "Reconstruction of conductivity and current density images using only one component of magnetic field measurements," *IEEE Trans. Biomed. Eng.*, vol. 50, no. 9, pp. 1121-1124, 2003.

(2) Oh *et. al.*, "Conductivity and current density image reconstruction using harmonic B_z algorithm in MREIT," *Phys. Med. Biol.*, vol. 48, Sep., vol. 48, pp. 3101-3116, 2003.

(3) Seo *et al.*, "Reconstruction of current density distributions in axially symmetric cylindrical sections using one component of magnetic flux density: computer simulation study," *Physiol. Meas.*, vol. 24, pp. 565-577, 2003.

(4) Park *et al.*, "Electrical conductivity imaging using gradient B_z decomposition algorithm in magnetic resonance electrical impedance tomography (MREIT)," *IEEE Trans. Med. Imaging*, vol. 28, pp. 388-394, 2004.

(5) Park *et al.*, "Static conductivity imaging using variational gradient B_z algorithm in magnetic resonance electrical impedance tomography (MREIT)," *Physiol. Meas.*, vol. 25, pp. 257-269, 2004.

(6) Kwon *et al.*, "Electrical conductivity imaging using a variational method in B_z-based MREIT," *Inv. Prob.*, vol. 21, pp. 969-980, 2005.

Experimental MREIT Studies

- MRI scanner: 3T, 11T, 17T, and 9.4T
- Imaging objects: phantoms and animals
- Recessed electrodes
- Current source
- Pulse sequence: SE and GE
- Software: MREIT toolbox

MRI Scanner: 3T Scanner at IIRC

Imaging Objects

- Conductivity Phantoms
  - Saline
  - Agar
  - Polyacrylamide
  - Sponge
  - Cotton thread and fabric
  - Silk thread and fabric
  - Sausage, fruit, and vegetable
- Tissue Phantoms
  - Biological tissues
  - Agar gel
- Animals
  - Pig
  - Dog
  - Others
- Human

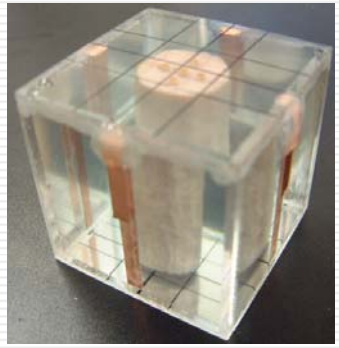
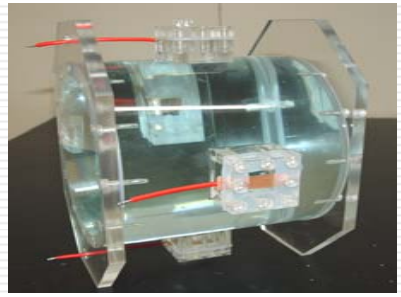

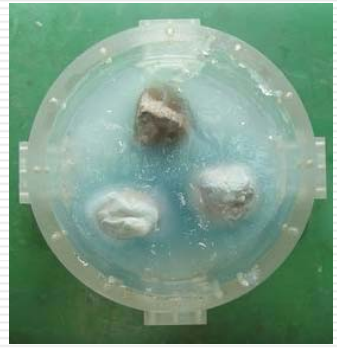
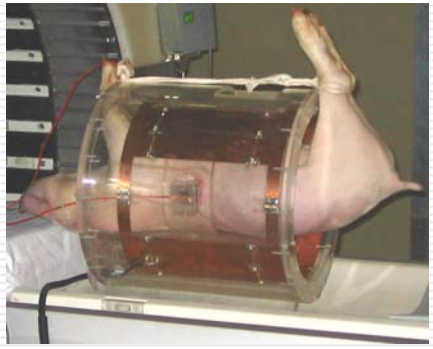


Recessed Electrodes

Phantom

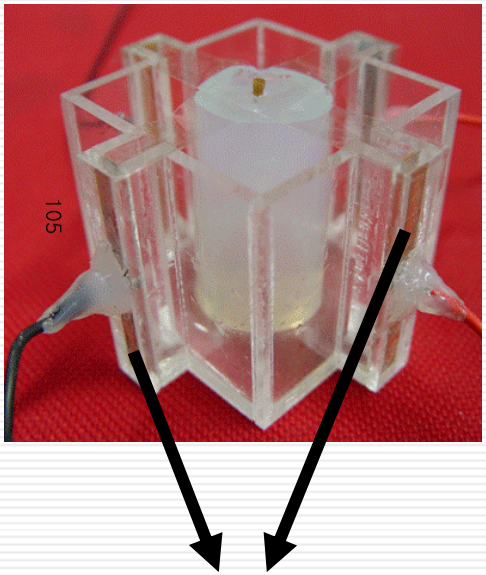

Recessed Electrodes

MR Magnitude Image

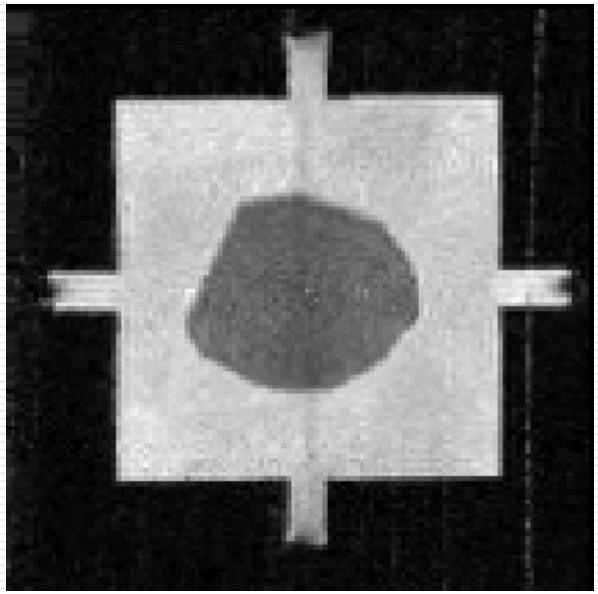

B_z Image

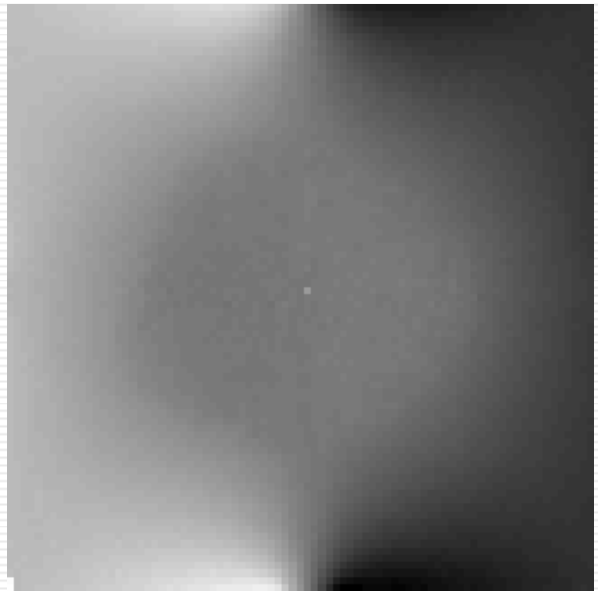

MREIT Current Source

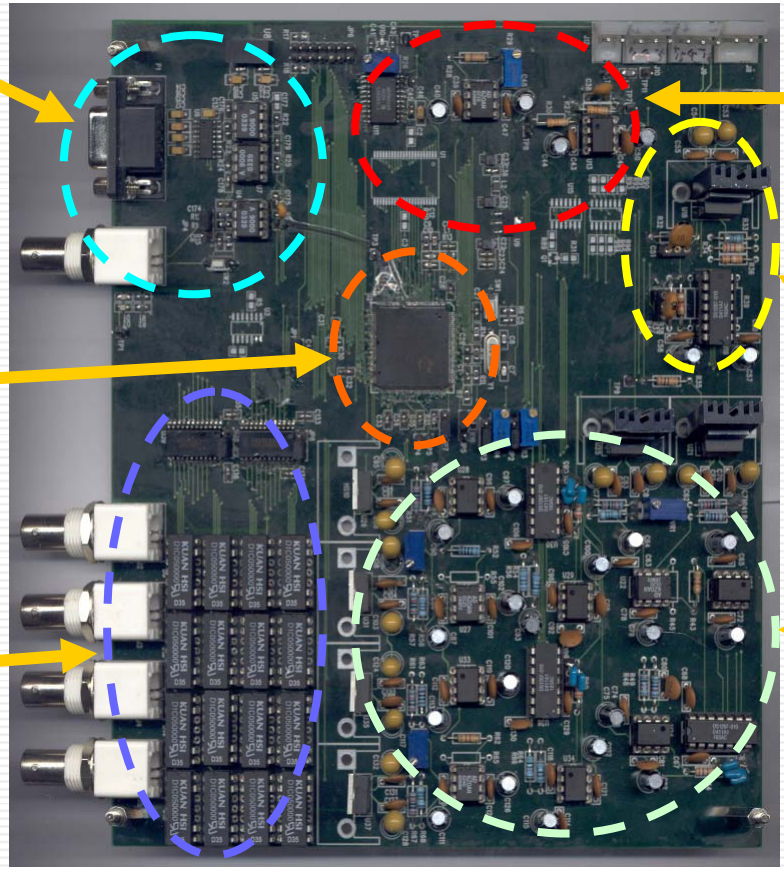

Agar Phantom: Setup

MRI parameters

TR/TE = 1400/60ms
FOV = 200mm
Matrix size = 128 ×128
Slice thickness/Gap = 3/0mm
Number of slices = 8
Average = 2
Current amplitude = 27mA
Current pulse width = 24ms
Voxel size(x,y,z) = 1.5625×1.5625×3mm^3

Phantom

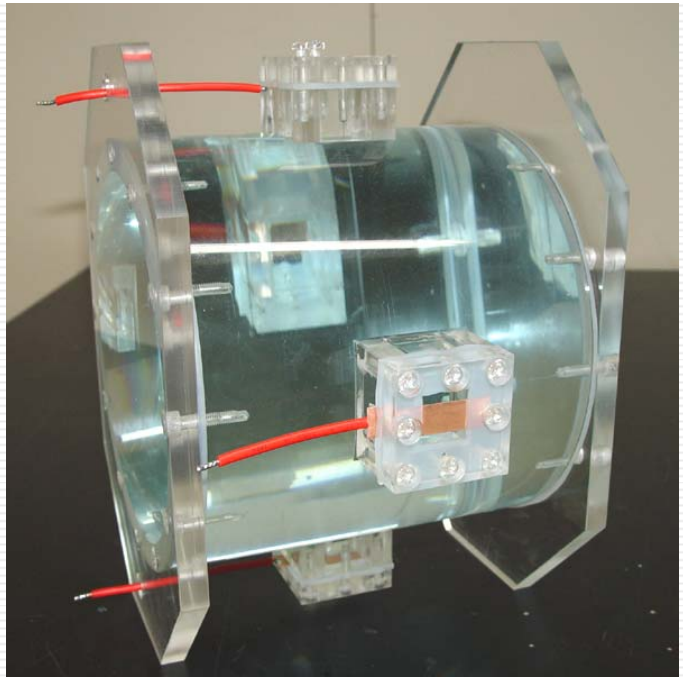

Phantom

Solution : 2S/m (NaCl=12.5g/l, $CuSO_4$=2g/l)
Object (agar) : 0.5S/m (NaCl=2g/l, $CuSO_4$=2g/l, Agar=15g/l)

Agar Phantom: *M* and Φ Images

Magnitude Image

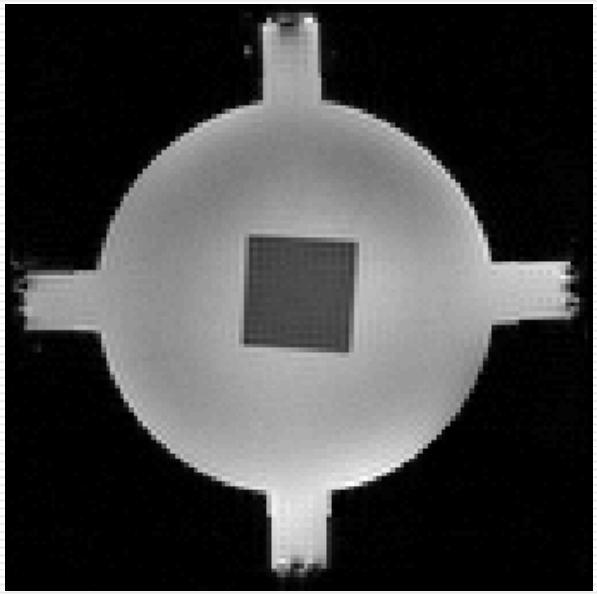

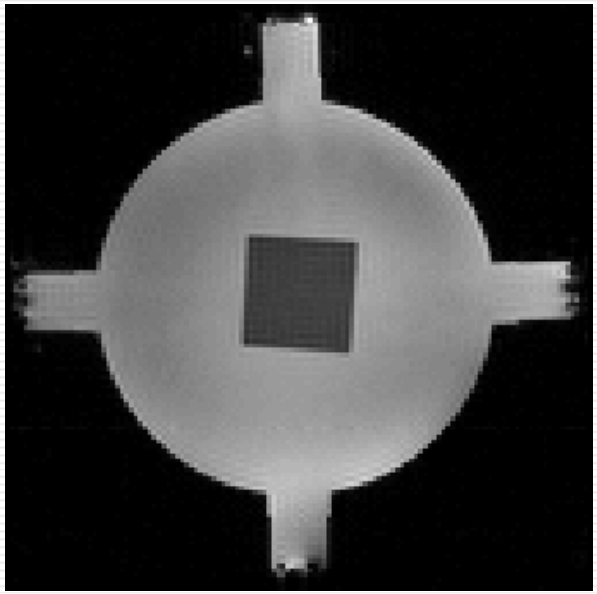

Wrapped Phase Image

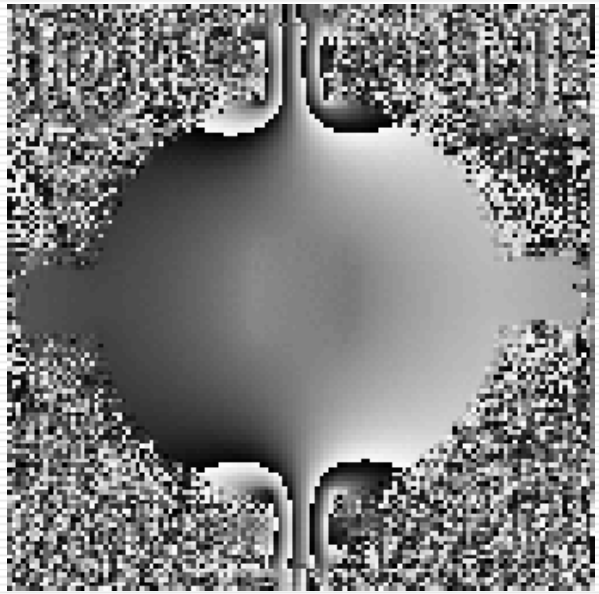

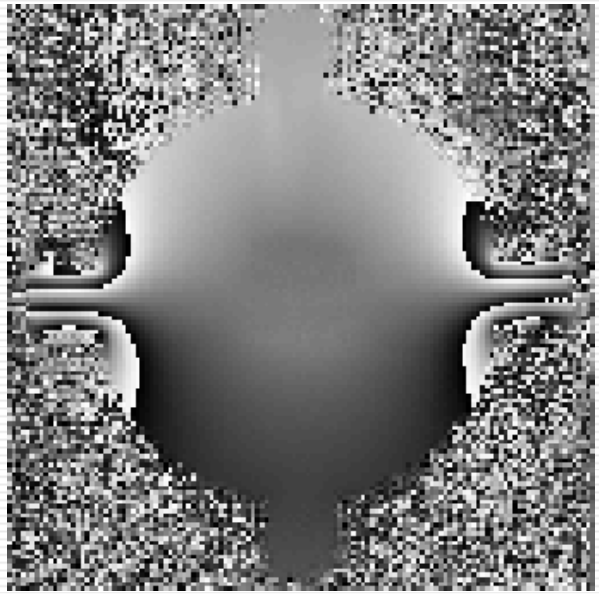

Agar Phantom: B_z Images

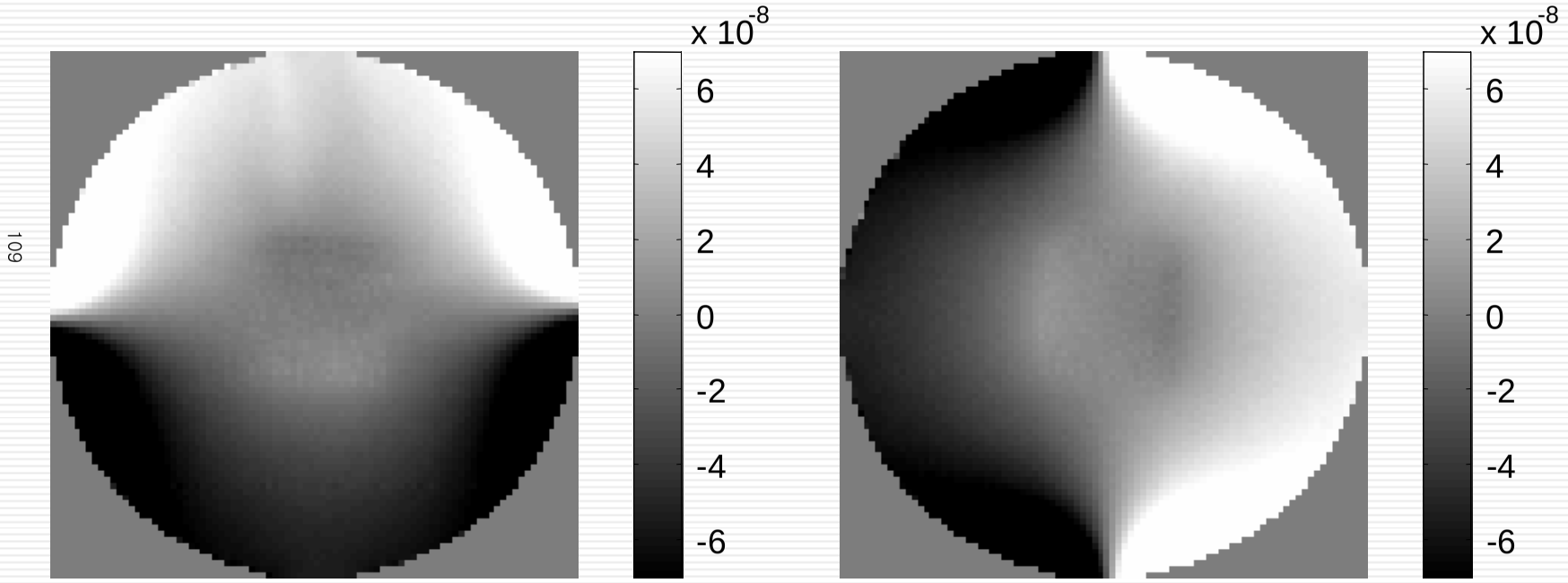

Horizontal Injection Current

Vertical Injection Current

Agar Phantom: σ Images

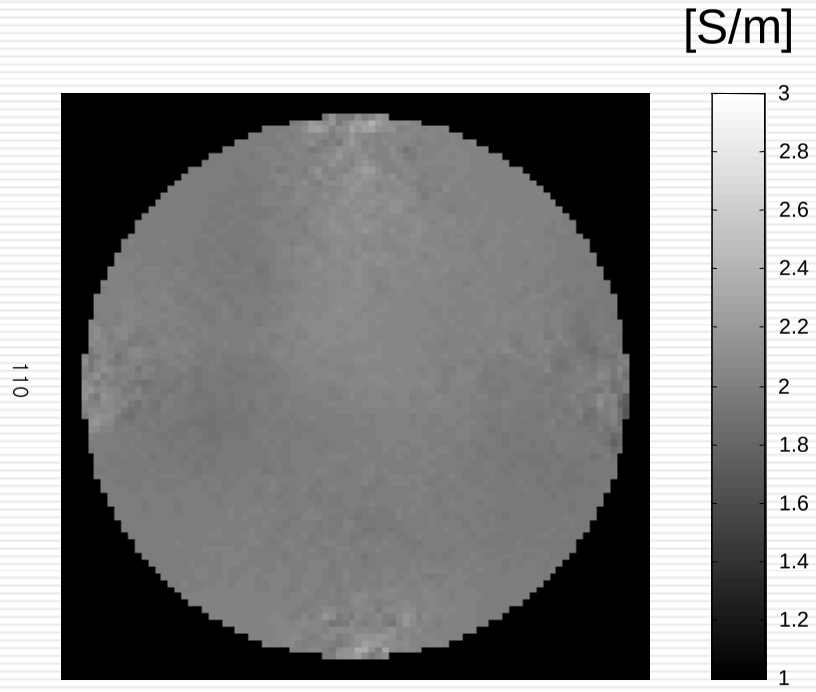

Homogeneous Phantom
(L^2-error = 3.2%)

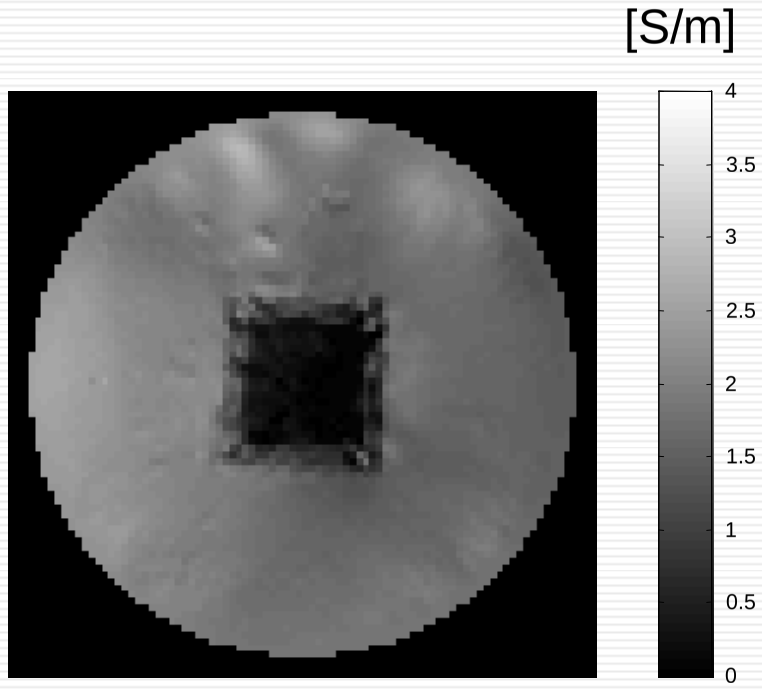

Agar Object Phantom
(L^2-error ~ 5%)

Resolution Phantom: Setup

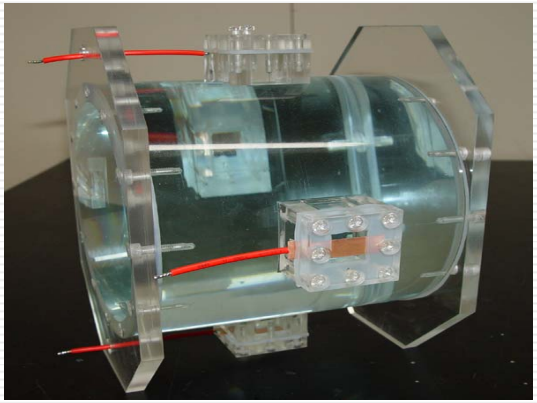

111

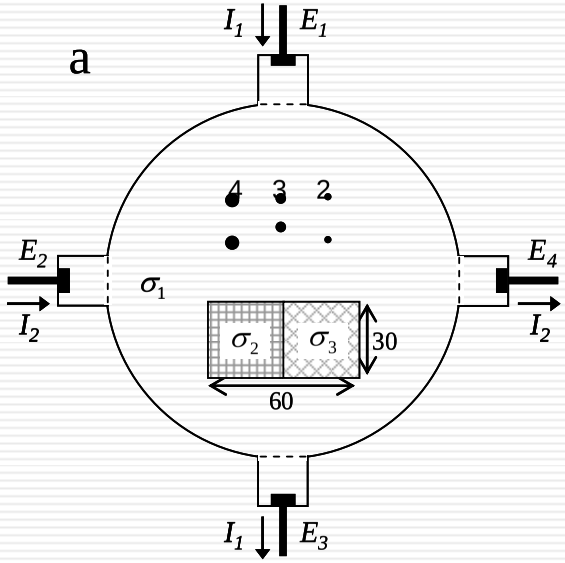

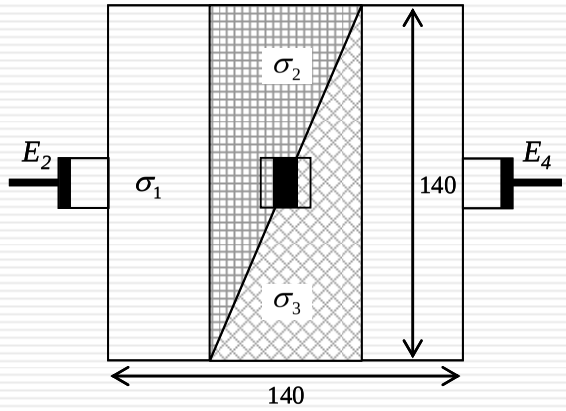

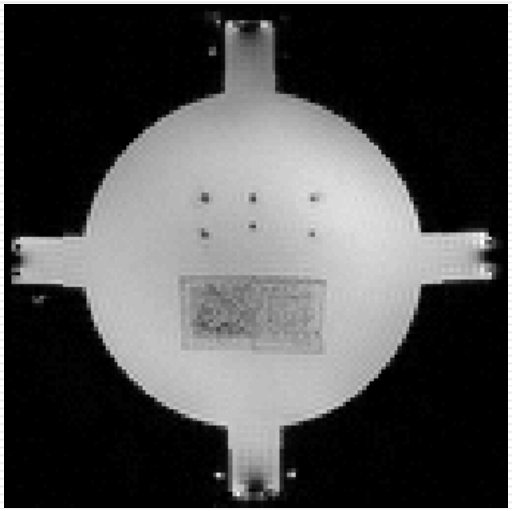

MR Magnitude Image

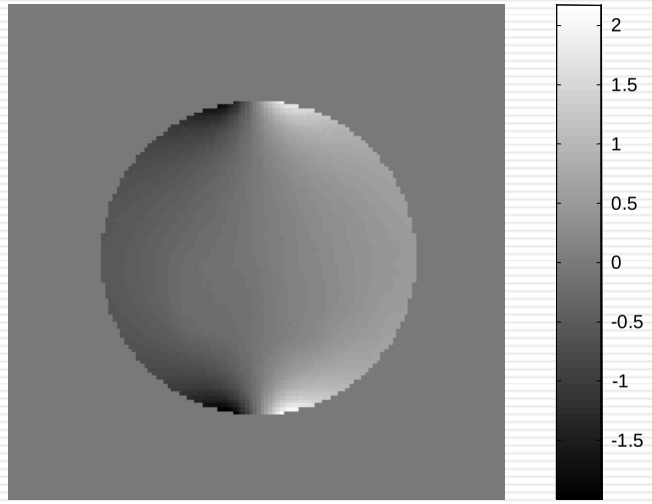

Magnetic Flux Density Image (B_z)

S. H. Oh, B. I. Lee, T. S. Park, S. Y. Lee, E. J. Woo, M. H. Cho, O. Kwon, and J. K. Seo, “Magnetic resonance electrical impedance tomography at 3 Tesla field strength,” *Mag. Reson. Med.*, 1292-1296, 2004.

Resolution Phantom: σ Images

MR Magnitude Image

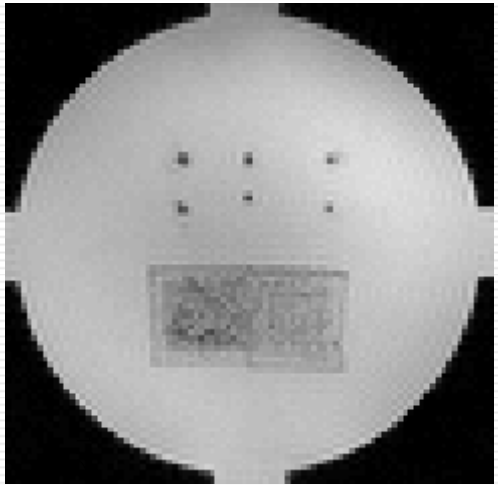

σ at slice #1

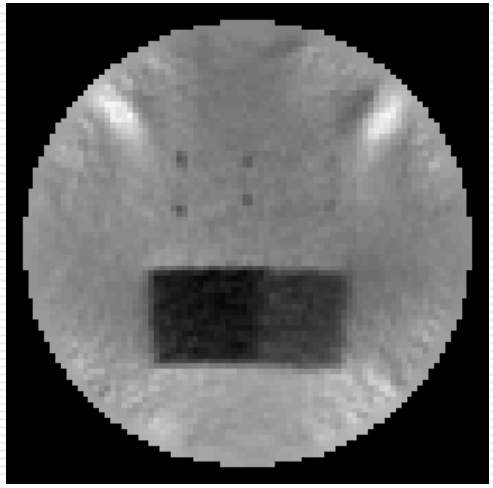

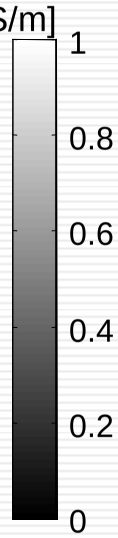

σ at slice #2

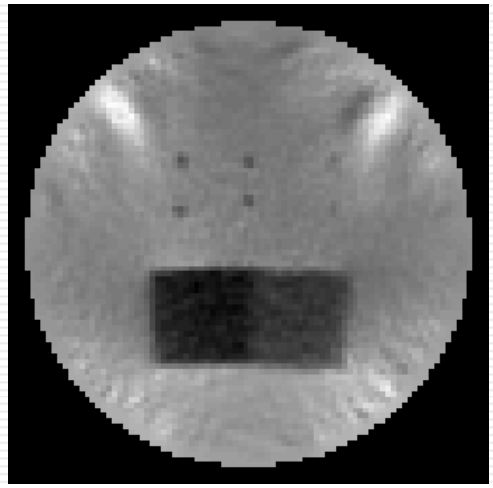

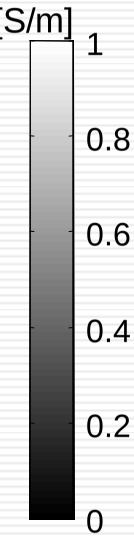

σ at slice #3

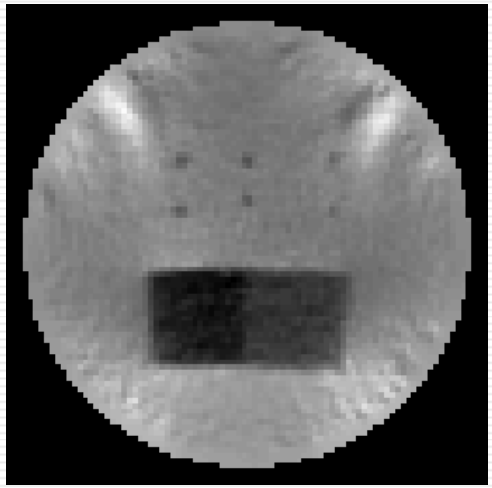

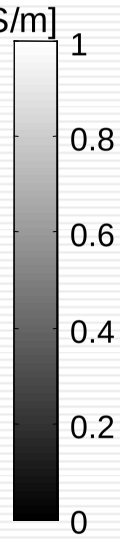

σ at slice #4

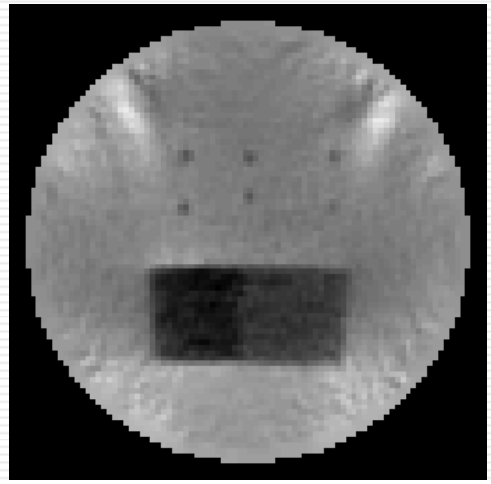

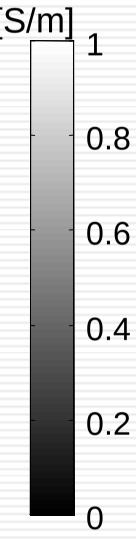

S. H. Oh, B. I. Lee, T. S. Park, S. Y. Lee, E. J. Woo, M. H. Cho, O. Kwon, and J. K. Seo, “Magnetic resonance electrical impedance tomography at 3 Tesla field strength,” *Mag. Reson. Med.*, 1292-1296, 2004.

Tissue Phantom: Setup

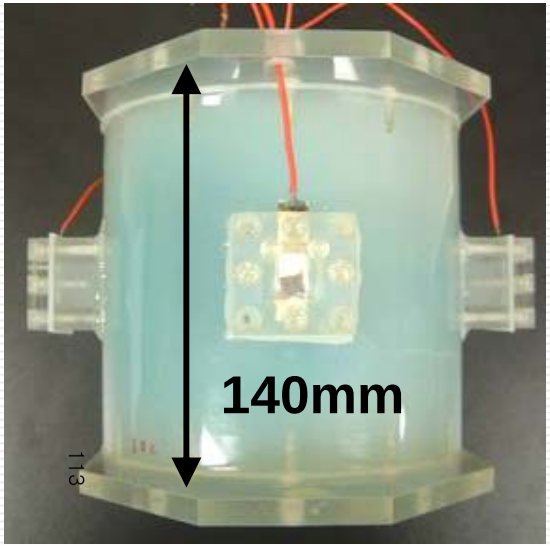

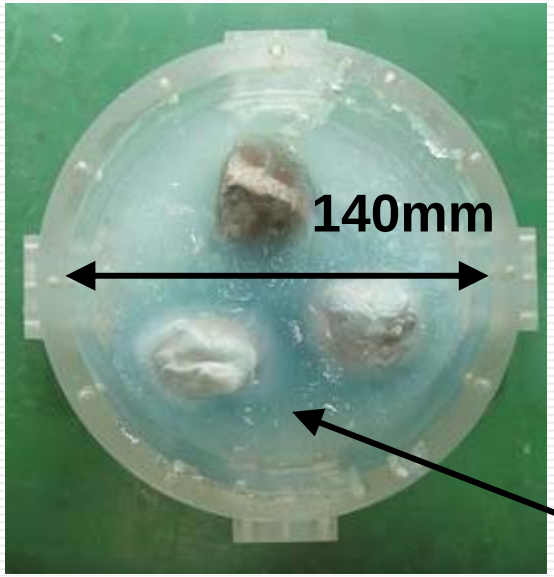

Chicken Breast Porcine Muscle Bovine Tongue

Tissue	Conductivity [S/m]	
	Longitudinal	Transversal
Chicken Breast	0.60	0.55
Bovine Tongue	0.41	0.36
Porcine Muscle	0.64	0.55
Bovine Liver	0.69	0.69
Agar Gelatin	0.76	0.76

Conductivity values were measured after experiments by an impedance analyzer using the four-electrode method.

Agar Gelatin (1g/l $CuSO_4$, 3.125 g/l NaCl, 7g/l Agar)

Tissue Phantom: B_z Images

M

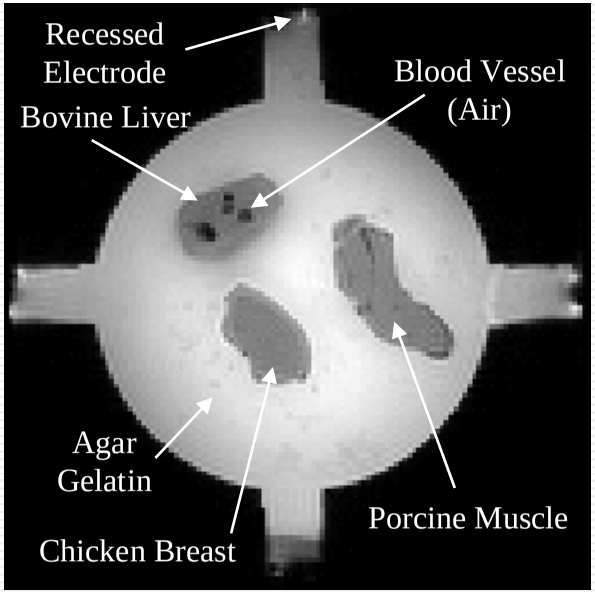

B_z

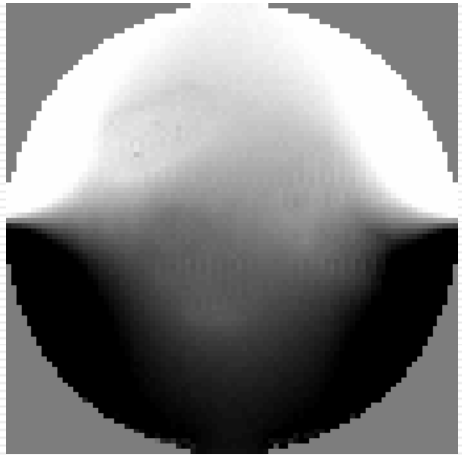

B_z

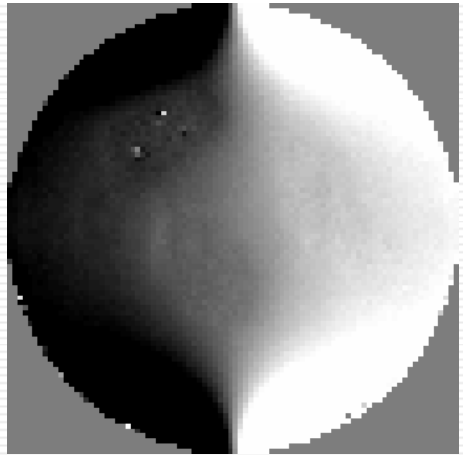

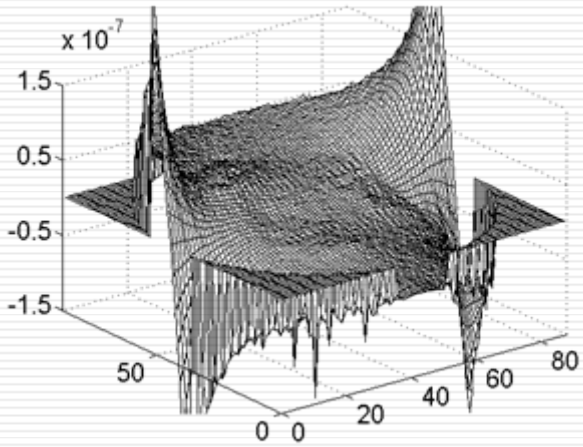

Horizontal Injection

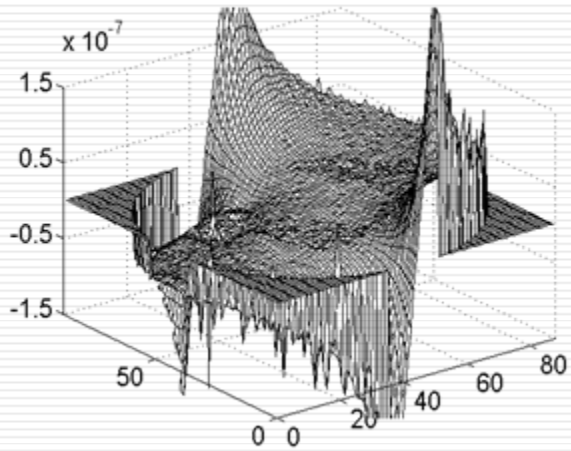

Vertical Injection

Tissue Phantom: B_z Images

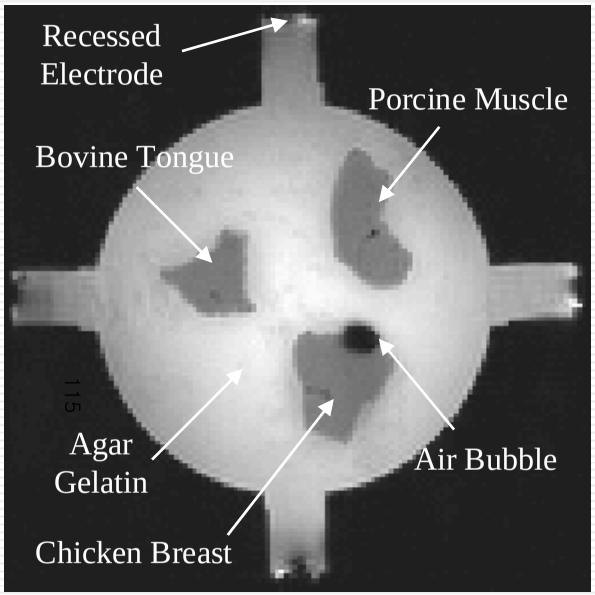

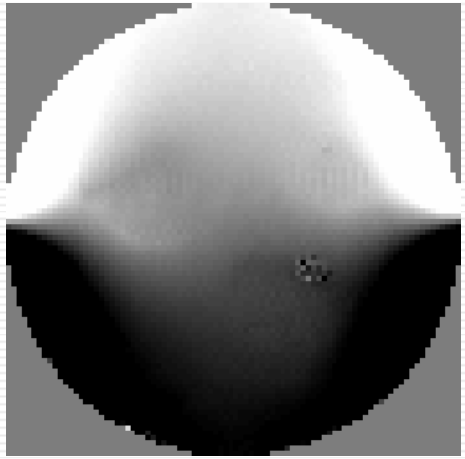

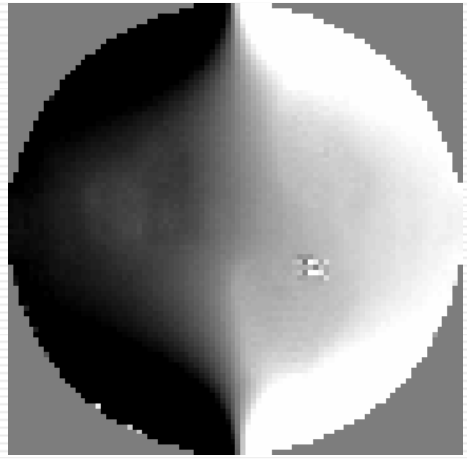

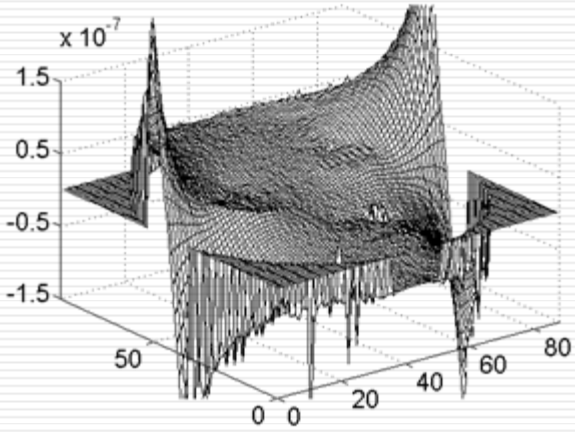

Horizontal Injection

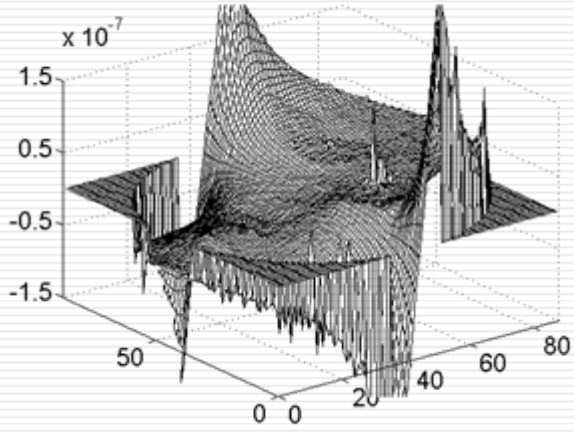

Vertical Injection

Tissue Phantom: σ Image

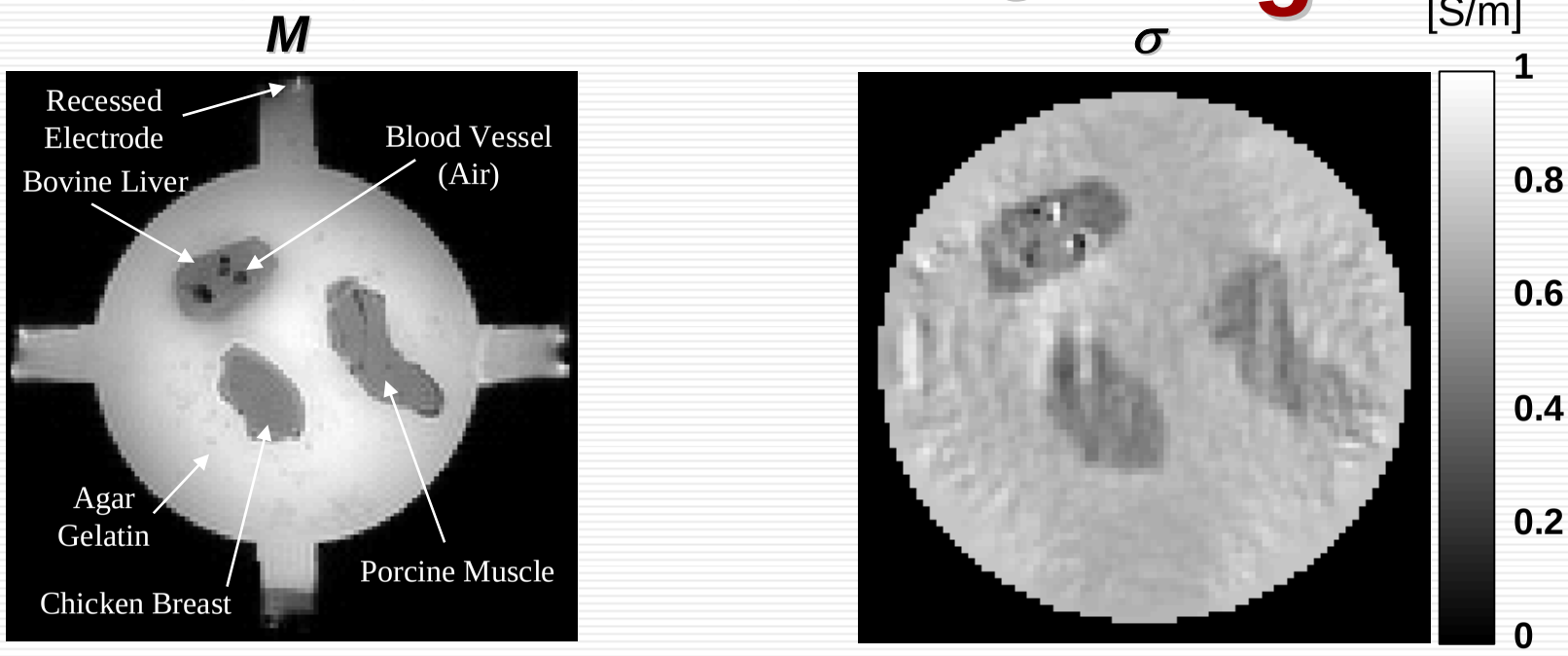

Tissue	Measured Conductivity [S/m]	Reconstructed Conductivity [S/m]
Agar Gelatin	0.76	0.73
Bovine Liver	0.69	0.64
Porcine Muscle	0.55 – 0.64	0.59
Chicken Breast	0.55 – 0.60	0.54

S. H. Oh, B. I. Lee, E. J. Woo, S. Y. Lee, T. S. Kim, O. Kwon, and J. K. Seo, "Electrical conductivity images of biological tissue phantoms in MREIT," *Physiol. Meas.*, vol. 26, pp. S279-S288, 2005.

Tissue Phantom: σ Image

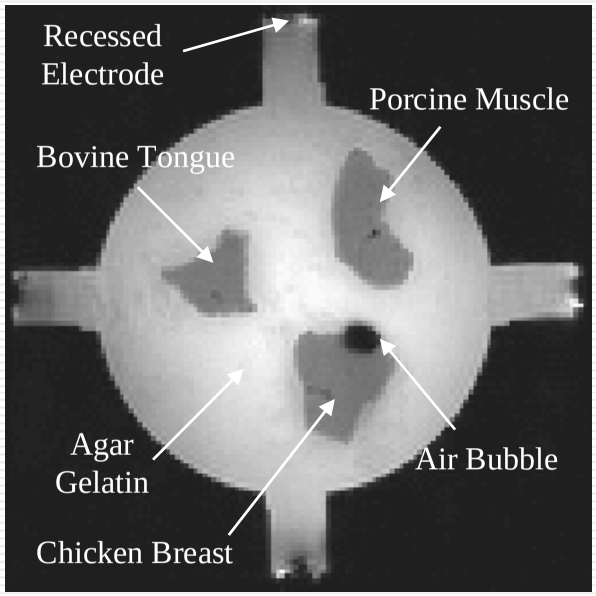

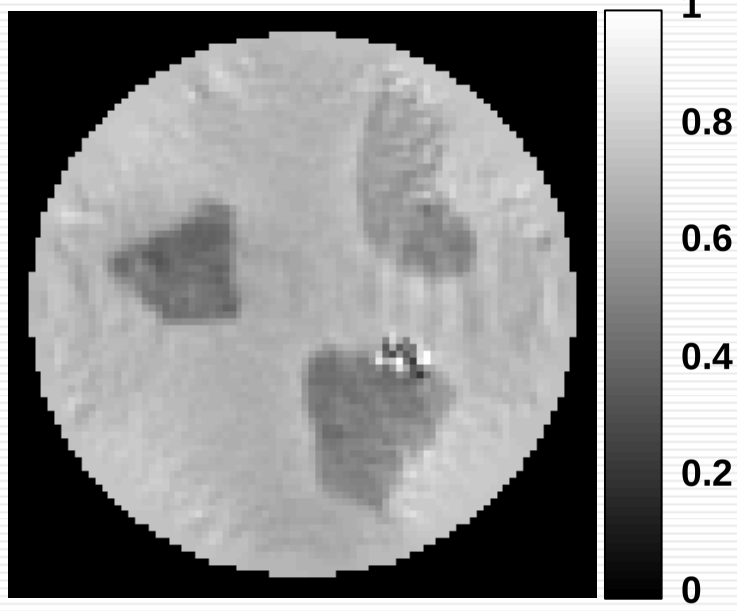

Tissue	Measured Conductivity [S/m]	Reconstructed Conductivity [S/m]
Agar Gelatin	0.76	0.73
Bovine Tongue	0.36 – 0.41	0.44
Porcine Muscle	0.55 – 0.64	0.59
Chicken Breast	0.55 – 0.60	0.52

S. H. Oh, B. I. Lee, E. J. Woo, S. Y. Lee, T. S. Kim, O. Kwon, and J. K. Seo, “Electrical conductivity images of biological tissue phantoms in MREIT,” *Physiol. Meas.*, vol. 26, pp. S279-S288, 2005.

Tissue Phantom: σ Images

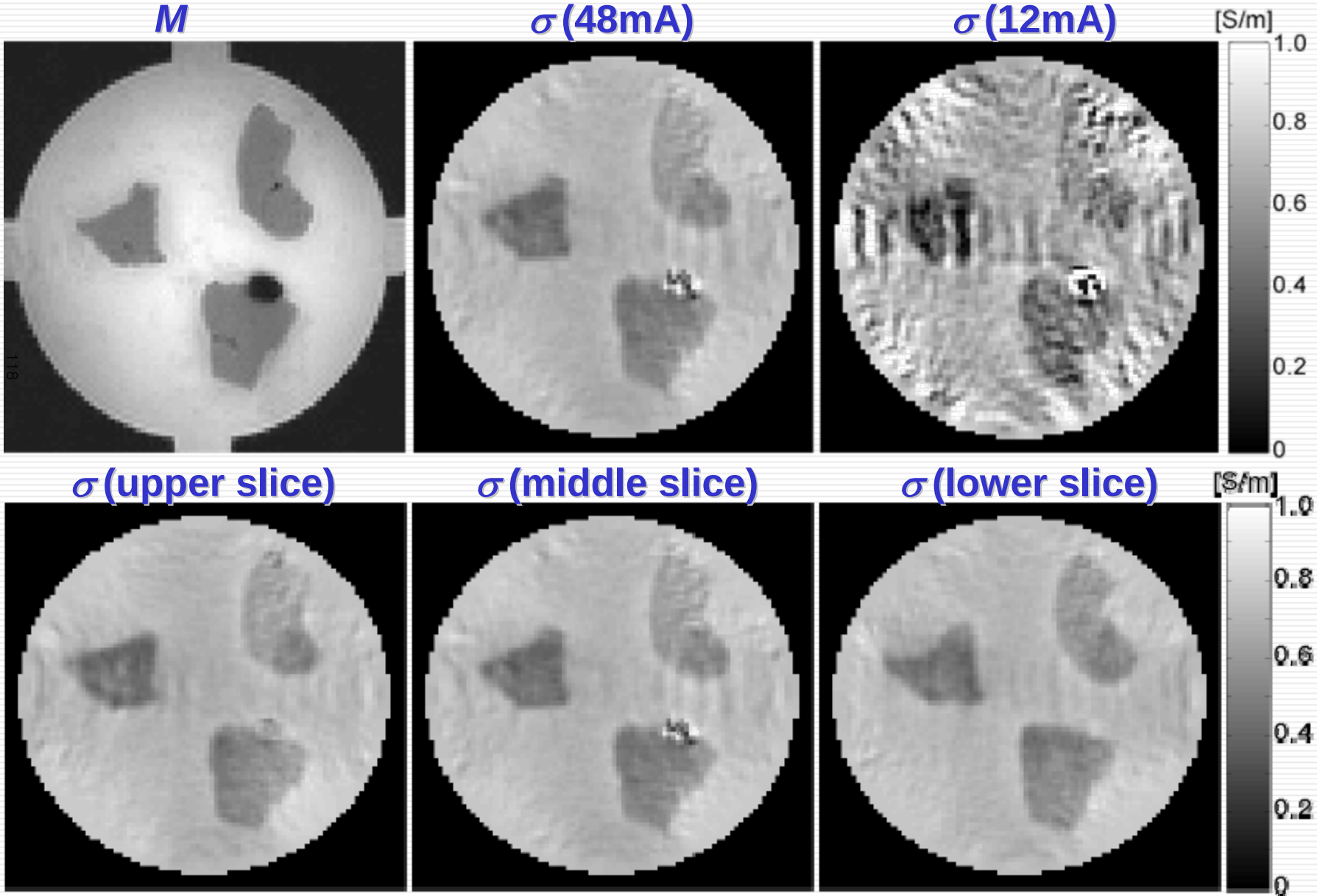

Estimation of the dielectric properties of biological materials at 100 Hz

Tissue	Conductivity [S/m]	Relative permittivity	Tissue	Conductivity [S/m]	Relative permittivity
Air	0	1	Fat	0.02081	457060
Aorta	0.27789	5.0921e+06	Gland	0.52211	492030
Blood	0.7	5259.8	Lymph	0.52211	492030
Blood Vessel	0.27789	5.0921e+06	Mucous Membrane	0.00046112	45298
Body Fluid	1.5	98.999	Muscle	0.26671	9.329e+06
Bone Cancellous	0.081031	217030	Nail	0.020059	5852.8
Bone Cortical	0.020059	5852.8	Nerve	0.028042	466020
Bone Marrow	0.001823	69898	Skin Dry	0.0002	1135.9
Breast Fat	0.023239	327610	Skin Wet	0.00046112	45298
Cartilage	0.17215	490460	Tendon	0.30479	1.1857e+07

Gabriel C et al, Phys. Med. Biol. 1996;41:2231-2293

http://niremf.ifac.cnr.it/tissprop/

Estimation of the dielectric properties of biological tissue at 100 Hz

Tissue	Conductivity [S/m]	Relative permittivity
Bladder	0.20558	192840
Brain Grey Matter	0.089018	3.9061e+06
Brain White Matter	0.058093	1.6677e+06
Cerebellum	0.10902	3.9064e+06
Cerebrospinal Fluid	2	109
Cervix	0.41134	2.0139e+07
Colon	0.12134	2.0091e+07
Dura	0.50056	19486
Gall Bladder	0.90001	1132
Gall Bladder Bile	1.4	120
Heart	0.093565	3.1637e+06
Kidney	0.10216	3.5181e+06
Lens	0.32216	590870
Liver	0.03813	678470
Lung Deflated	0.20588	567080
Lung Inflated	0.072979	1.7724e+06
Oesophagus	0.52211	491530
Ovary	0.32211	487140
Pancreas	0.52211	492030
Prostate	0.42211	494530
Retina	0.50283	146960
Small Intestine	0.52241	873130
Spinal Cord	0.028042	466020
Spleen	0.095662	3.1174e+06
Stomach	0.52211	491530
Testis	0.42211	494530
Thyroid	0.52211	492030
Tongue	0.27211	493520
Tooth	0.020059	5852.8
Uterus	0.29009	2.4512e+07

Gabriel C et al, Phys. Med. Biol. 1996;41:2231-2293

http://niremf.ifac.cnr.it/tissprop/

Dielectric anatomical model of permittivity and conductivity at 120 MHz and 1 GHz

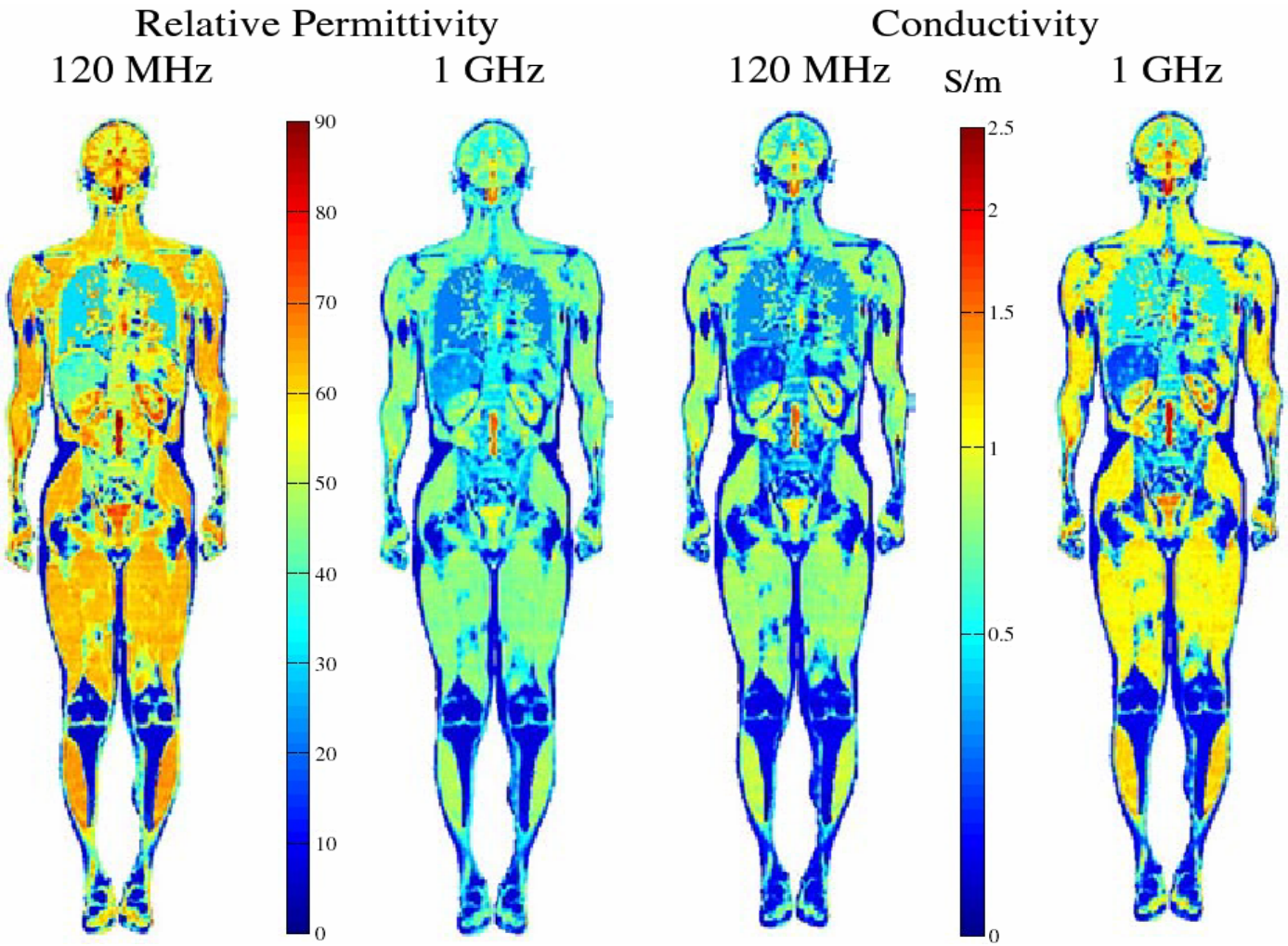

Mazzurana M et al, Phys. Med. Biol. 2003;48:3157-3170

Animal Experiment: Setup

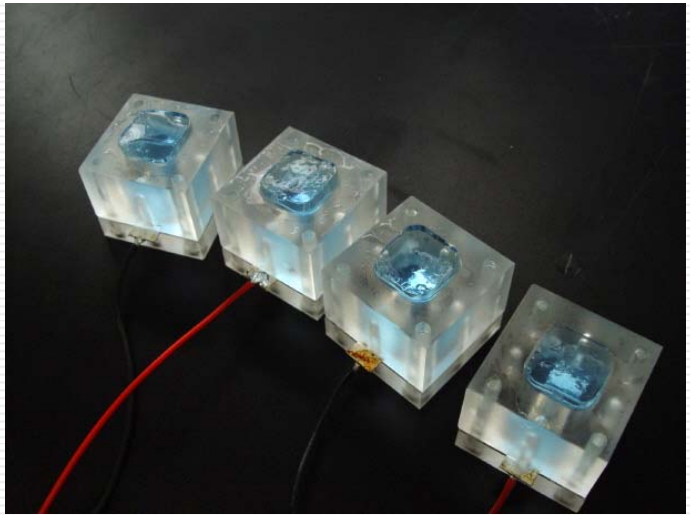

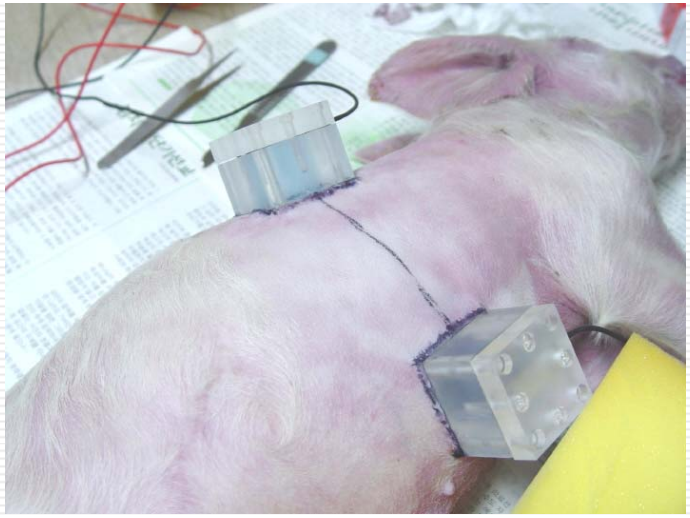

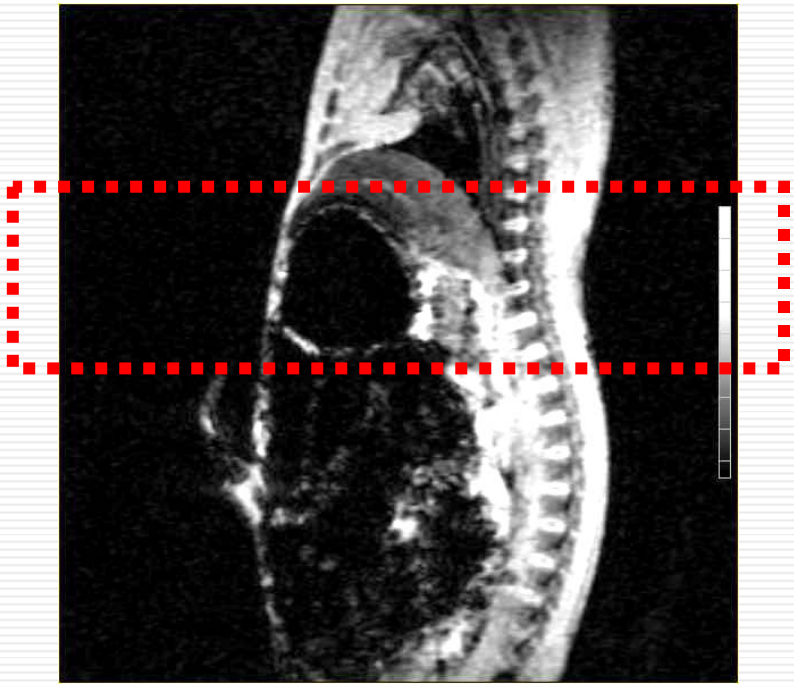

Animal Experiment: Pre-processing

MR Image

Pre-processing

- Shape extraction
  - Boundary
  - Electrode position
- Phase unwrapping
- Meshing
- Extraction of interior regions with very low SNR in B_z
- B_z data filling by $\nabla^2 B_z = 0$

Animal Experiment: B_z Images

MR Magnitude Image

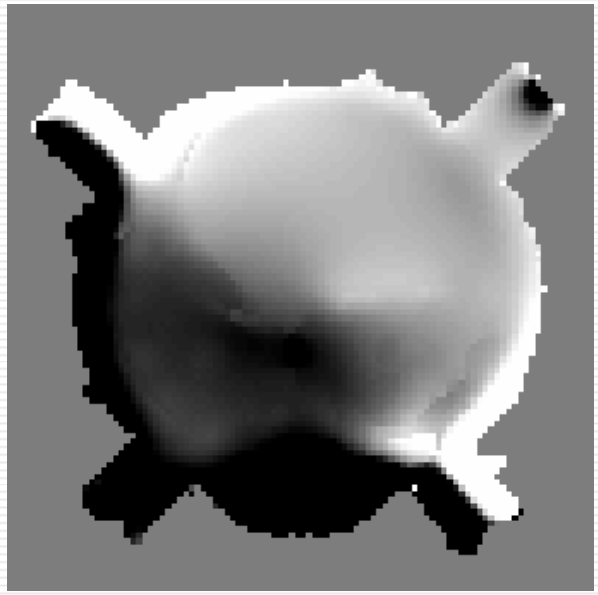

B_z Image

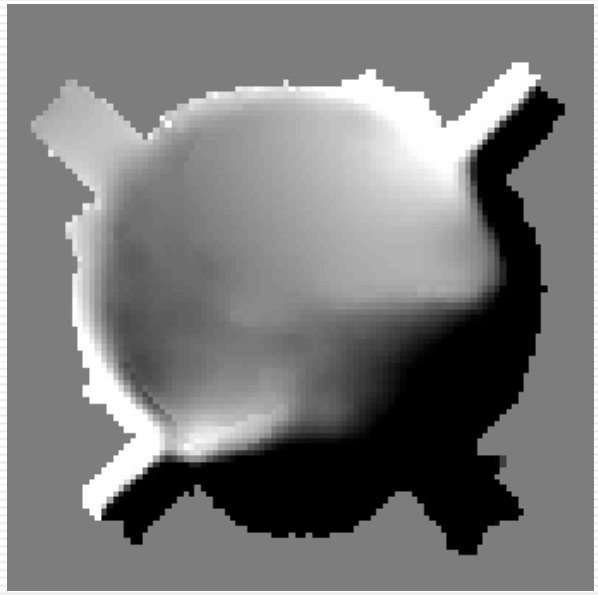

B_z Image

Animal Experiment: σ Image

MR Magnitude Image

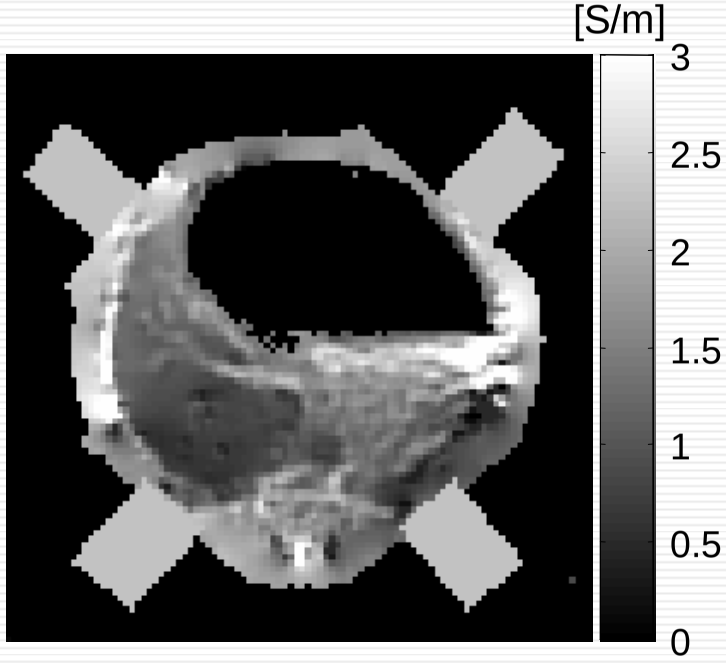

Conductivity Image

Animal Experiment: Subject

1) Weight : 11Kg
2) Length : about 700mm
3) Diameter (chest): about 150mm

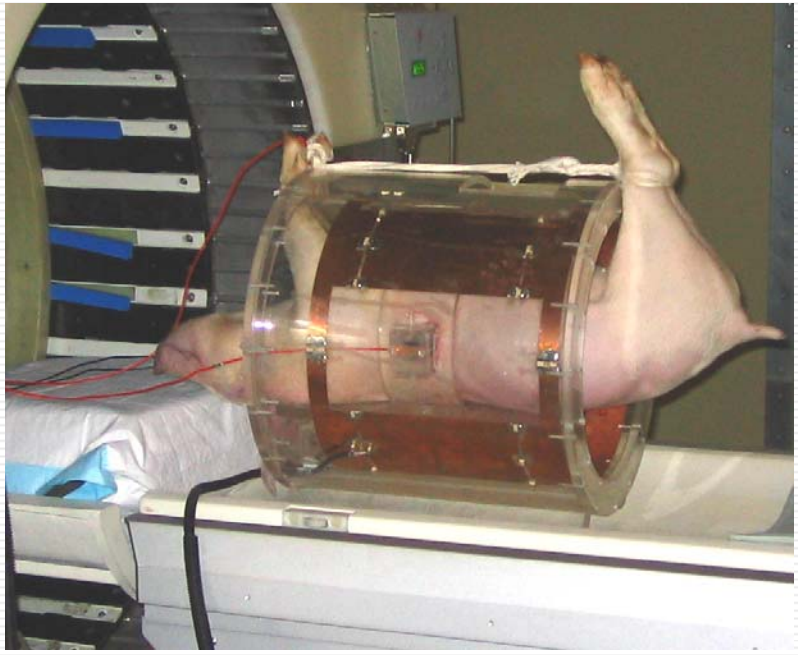

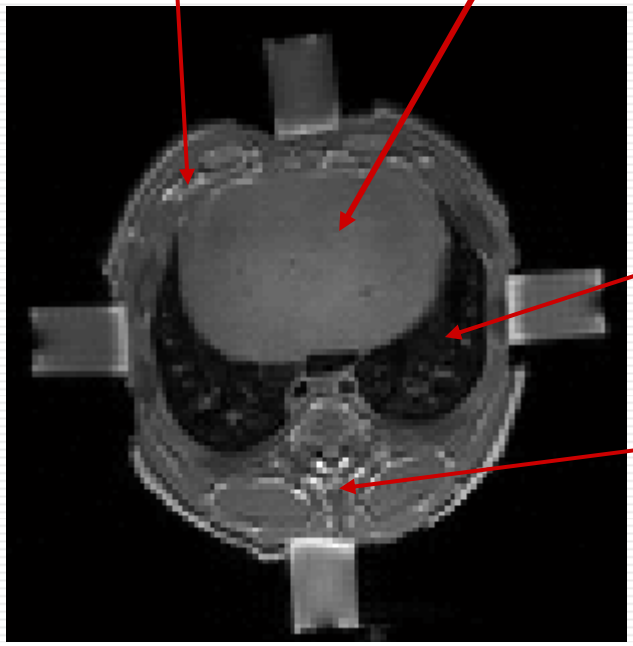

Animal Experiment: B_z Image

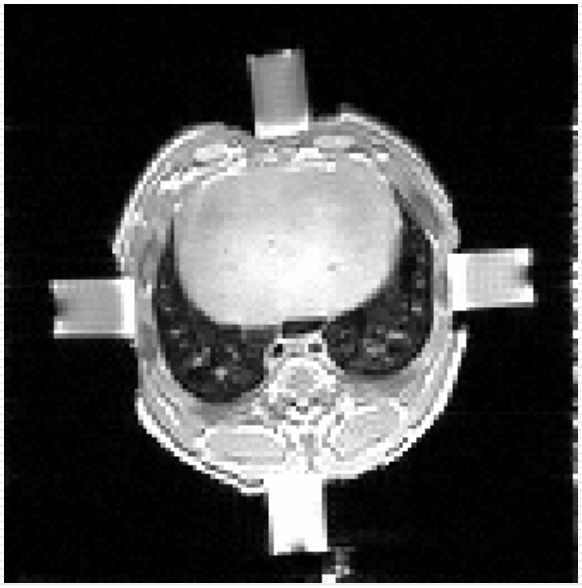

MR Magnitude Image

B_z for Horizontal Injection

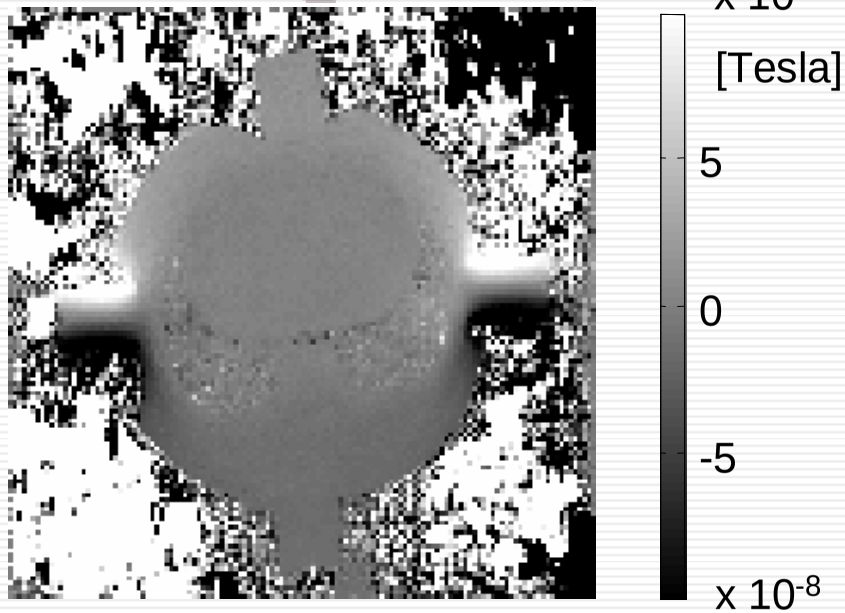

B_z for Vertical Injection

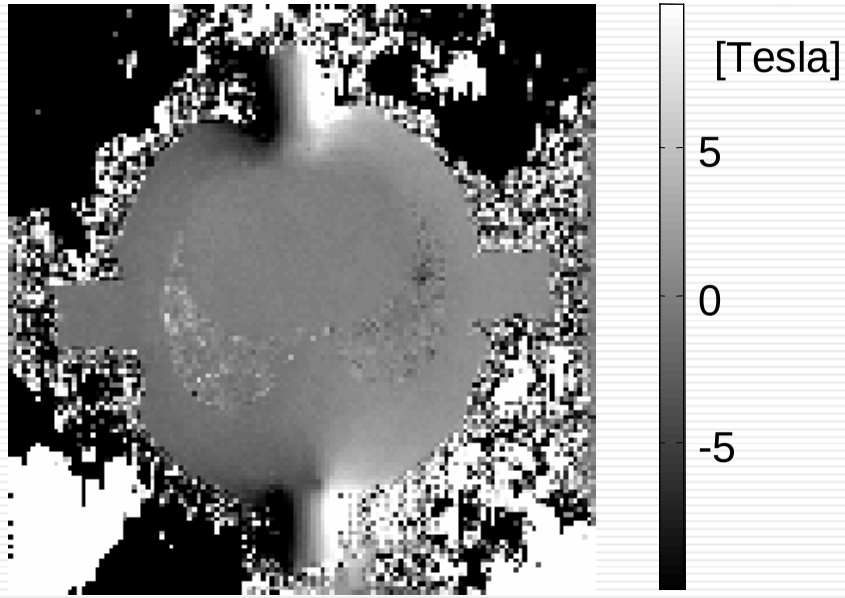

Animal Experiment: σ Image

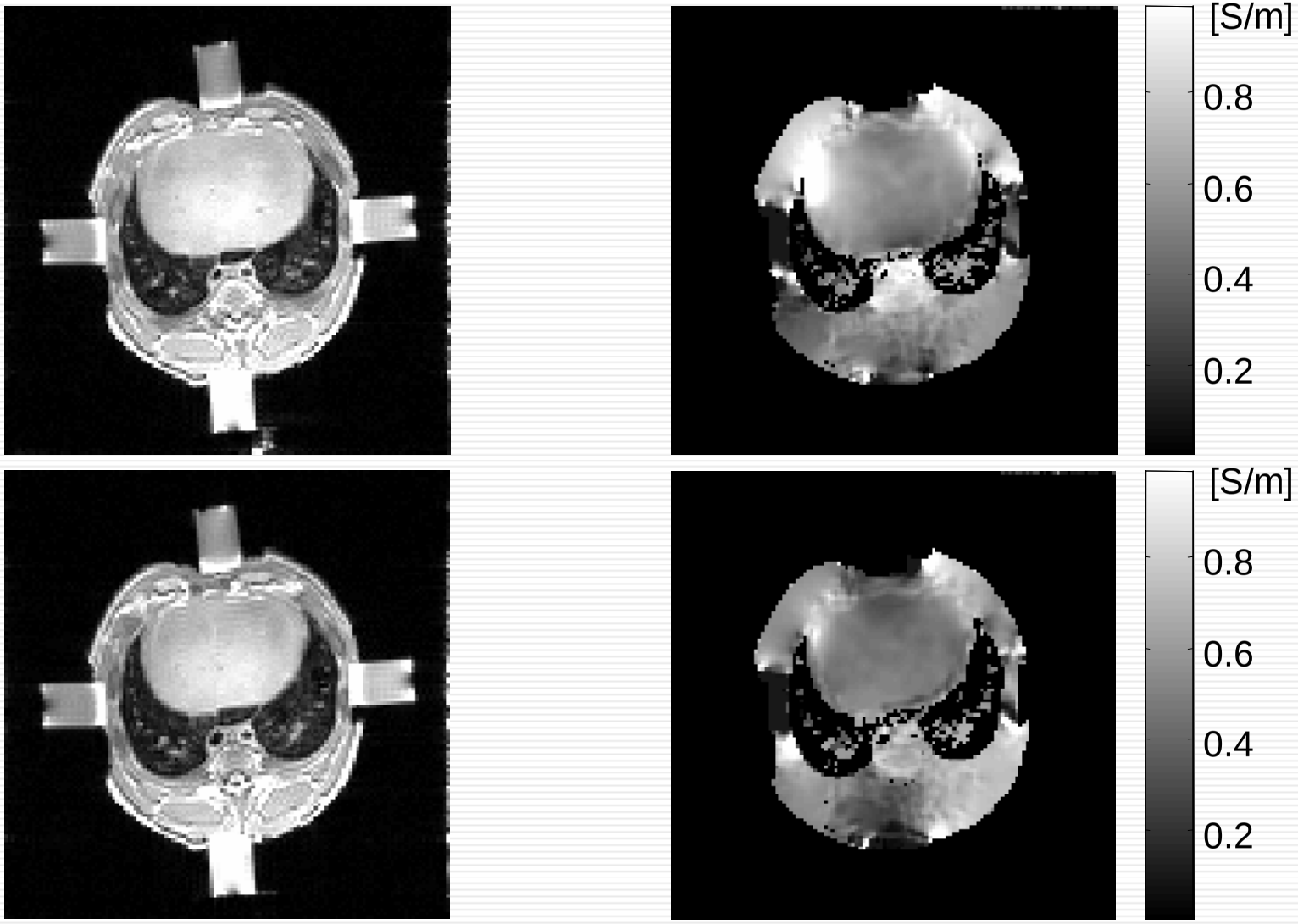

MR Magnitude Image

Conductivity Image